Table 1 Cases used for histological and immunohistochemical analysis

Case number	Age	Gender	Neuropathological diagnosis	CDR score	Aβ-MTL phase	Braak-NFT stage	CERAD-plaque score	NIA-AA AD degree	Biochemical-Aβ stage analogue for plaques
A1	62	M	Control	0	0	0	0	Not AD	0
A2	62	M	Control	0	0	0	0	Not AD	0
A3	66	F	Control	0	0	0	0	Not AD	0
A4	61	M	Control	0	0	0	0	Not AD	0
A5	69	F	Control	0	0	0	0	Not AD	0
A6	66	M	Control	0	0	1	0	Not AD	0
A7	72	F	Control	0	0	1	0	Not AD	0
A8	66	M	Control	0	0	1	0	Not AD	0
A9	60	M	Control	0	0	1	0	Not AD	0
A10	74	M	Control	0	0	1	0	Not AD	0
A11	71	M	p-preAD	0	2	1	0	Low	2
A12	64	M	p-preAD	0	2	1	0	Low	2
A13	83	M	p-preAD, brain infarction	0	2	3	0	Low	1
A14	72	M	p-preAD	0	2	3	0	Low	2
A15	71	M	p-preAD, brain infarction	0	3	1	0	Low	1
A16	84	F	p-preAD, brain infarction	0	3	3	0	Intermediate	3
A17	87	M	p-preAD	0	3	3	1	Intermediate	3
A18	83	F	p-preAD	0	3	3	1	Intermediate	3
A19	63	F	p-preAD, brain infarction	0	4	3	1	Intermediate	2
A20	85	F	p-preAD	0	4	3	1	Intermediate	2
A21	66	F	p-preAD	n.d.	2	2	0	Low	2
A22	86	M	p-preAD, VD	0.5	2	2	0	Low	1
A23	88	M	p-preAD, AGD	2	3	2	1	Low	3
A24	78	M	AD	1	3	4	1	Intermediate	3
A25	68	F	AD	1	4	6	3	High	3
A26	82	M	AD	2	3	3	2	Intermediate	3
A27	89	F	AD	2	4	4	3	Intermediate	3
A28	87	F	AD	3	4	4	1	Intermediate	3
A29	83	M	AD	3	4	4	2	Intermediate	3
A30	81	F	AD	3	4	5	1	Intermediate	3
A31	89	F	AD	3	4	5	2	High	3
A32	78	F	AD	3	4	5	3	High	3
A33	83	M	AD	3	4	5	3	High	3
A34	86	F	AD, AGD	3	4	6	3	High	3

Age in years. Clinical dementia rating (CDR) scores (Morris, 1993), Aβ-MTL phase (Thal *et al.*, 2000), Braak–neurofibrillary tangle stage (Braak *et al.*, 2006), CERAD score for neuritic plaque density (Mirra *et al.*, 1991), and the degree of Alzheimer's disease pathology (Hyman *et al.*, 2012) were determined as previously published and recommended. The biochemical Aβ stage was determined as depicted in Fig. 6. M = male; F = female, (control) non-demented control; AD = Alzheimer's disease; AGD = argyrophilic grain disease; ALS = amyotrophic lateral sclerosis; CBD = corticobasal degeneration; FTLD-TDP = frontotemporal lobar degeneration with TDP43-pathology; MCI (AD) = mild cognitive impairment with predominant Alzheimer's disease pathology; MTL = medial temporal lobe; n.d. = not done; NIA-AA AD degree = Degree of Alzheimer's disease pathology (Hyman *et al.*, 2012); NFT = neurofibrillary tangle; NMO = neuromyelitis optica; p-preAD = pathologically diagnosed preclinical Alzheimer's disease; VD = vascular dementia.

(Tables 1 and 2). None of the investigated cases had a known familial background for Alzheimer's disease. After autopsy, brains were fixed in a 4% aqueous solution of formaldehyde. Following fixation the medial temporal lobe and tissue from the occipital cortex containing the primary visual field were embedded in paraffin. Further medial temporal lobe tissue of the cases listed in Table 1 was embedded in polyethylene glycol. Paraffin sections were cut at 12 μm, polyethylene glycol sections at 100 μm. Histopathological diagnosis of Alzheimer's disease was performed by analysing Gallyas, Campbell-Switzer, anti-abnormal tau-protein (anti-PHF-τ) and anti-$A\beta_{17-24}$ stained sections of the medial temporal lobe and the occipital cortex (Supplementary Table 1). Braak neurofibrillary tangle staging and the assignment of Consortium to Establish a Registry for Alzheimer's Disease (CERAD) scores for neuritic plaque density were performed on the basis of the Gallyas-stained and anti-PHF-τ-stained sections (Braak and Braak, 1991; Mirra *et al.*, 1991; Braak *et al.*, 2006; Alafuzoff *et al.*, 2008). The distribution of amyloid plaques in the medial temporal lobe (Aβ–medial temporal lobe phase) had been obtained according to previously published criteria (Thal *et al.*, 2000) and represents the distribution of Aβ plaques in the human brain as a semi-quantitative parameter for the overall severity of Aβ plaque pathology (Thal *et al.*, 2002). Aβ–medial temporal lobe phase, Braak–neurofibrillary tangle stages and CERAD scores for neuritic plaques were used to determine the degree of Alzheimer's disease pathology according to recently published guidelines (Hyman *et al.*, 2012).

The cases had usually been examined 1 to 4 weeks before death by different clinicians according to standardized protocols. The protocols included the assessment of cognitive function and recorded the ability

Table 2 Cases used for histological, immunohistochemical and for biochemical analysis from frozen neocortex samples

Case number	Age	Gender	Neuropathological diagnosis	CDR Score	Aβ-MTL phase	Braak-NFT stage	CERAD-plaque score	NIA-AA – AD degree	Biochemical-Aβ stage	Biochemical-Aβ stage analogue for plaques
B1	60	M	Control	0	0	0	0	Not AD	0	0
B2	35	M	Limbic encephalitis	0	0	0	0	Not AD	0	0
B3	45	M	Control	0	0	0	0	Not AD	0	0
B4	58	F	Control	0	0	0	0	Not AD	0	0
B5	66	M	Control	0	0	1	0	Not AD	0	0
B6	69	F	Control	0	0	1	0	Not AD	0	0
B7	71	F	Control	0	0	1	0	Not AD	0	0
B8	46	M	Control	0	0	1	0	Not AD	0	0
B9	59	M	Control	n.d.	0	1	0	Not AD	0	0
B10	57	M	Control	0	0	1	0	Not AD	0	0
B11	53	M	p-preAD	0	1	1	0	Low	0	2
B12	72	M	p-preAD, NMO	0	1	1	0	Low	1	2
B13	78	F	p-preAD, VD, CBD	3	1	1	0	Low	0	2
B14	73	F	p-preAD	0	1	2	0	Low	3	2
B15	72	F	p-preAD	0	1	2	0	Low	0	2
B16	73	F	p-preAD	0	1	2	0	Low	0	2
B17	68	F	p-preAD	0	2	1	0	Low	2	2
B18	64	M	p-preAD, Brain infarction	n.d.	2	1	0	Low	2	2
B19	82	F	p-preAD, metastatic lung carcinoma, *microinfarcts*	n.d.	2	1	1	Low	2	2
B20	68	F	p-preAD	0	2	2	0	Low	2	3
B21	74	M	p-preAD	0	2	2	0	Low	0	2
B22	67	F	p-preAD	0	2	2	0	Low	2	2
B23	77	F	p-preAD, VD	3	2	3	1	Low	0	2
B24	73	F	p-preAD	n.d.	3	1	0	Low	3	3
B25	84	F	p-preAD	0	3	2	0	Low	2	3
B26	77	F	p-preAD	0	3	2	0	Low	3	3
B27	78	F	p-preAD	0	3	2	0	Low	2	3
B28	71	M	p-preAD	0	3	2	1	Low	2	3
B29	71	F	p-preAD	0	3	2	1	Low	1	2
B30	74	M	p-preAD	0	4	3	1	Intermediate	3	3
B31	91	F	AD	3	3	4	1	Intermediate	3	n.d.
B32	79	F	AD	n.d.	3	4	2	Intermediate	3	3
B33	84	M	AD, AGD, ALS, VD	3	3	4	2	Intermediate	3	3
B34	75	F	MCI (AD)	0.5	4	3	1	Intermediate	3	3
B35	78	M	AD	3	4	4	1	Intermediate	3	3
B36	72	F	AD	1	4	4	2	Intermediate	3	3
B37	83	M	AD	1	4	4	2	Intermediate	3	3
B38	64	F	AD	n.d.	4	6	3	High	3	3
B39	62	F	AD	3	4	6	3	High	3	3
B40	84	M	AD	3	4	6	3	High	3	3

Age in years. Clinical dementia rating (CDR) scores (Morris, 1993), Aβ–medial temporal lobe phase (Thal *et al.*, 2000), Braak–neurofibrillary tangle stage (Braak *et al.*, 2006), CERAD score for neuritic plaque density (Mirra *et al.*, 1991), and the degree of Alzheimer's disease pathology (Hyman *et al.*, 2012) were determined as previously published and recommended. The biochemical Aβ stage was determined as depicted in Fig. 6. M = male; F = female, (control) non-demented control; AD = Alzheimer's disease; AGD = argyrophilic grain disease; ALS = amyotrophic lateral sclerosis; CBD = corticobasal degeneration; FTLD-TDP = frontotemporal lobar degeneration with TDP43-pathology; MCI (AD) = mild cognitive impairment with predominant Alzheimer's disease pathology; MTL = medial temporal lobe; n.d. = not done; NIA-AA AD degree = Degree of Alzheimer's disease pathology (Hyman *et al.*, 2012); NFT = neurofibrillary tangle; NMO = neuromyelitis optica; p-preAD = pathologically diagnosed preclinical Alzheimer's disease; VD = vascular dementia.

to care for and dress oneself, eating habits, bladder and bowel continence, speech patterns, writing and reading, short-term and long-term memory, and orientation within the hospital setting. In the event that a Clinical Dementia Rating score could not be obtained because of missing clinical data, this is noted in Table 1. These data were used to retrospectively assess Clinical Dementia Rating scores for each patient (Morris *et al.*, 1989). The diagnosis of symptomatic Alzheimer's disease including Alzheimer's disease-related mild cognitive impairment was considered for all individuals with a Clinical Dementia Rating score $\geqslant 0.5$, which exhibited either an intermediate or high degree of Alzheimer's disease pathology according to the National Institute of Aging Alzheimer Association (NIA-AA) guidelines for the neuropathological diagnosis of Alzheimer's disease (Hyman *et al.*, 2012). Controls were defined by the absence of any Aβ plaques. They either had no

neurofibrillary tangles or not more than Braak–neurofibrillary tangle stage I. Non-demented cases with Aβ plaques, i.e. having low or intermediate degrees of Alzheimer's disease pathology were categorized as cases with pathologically preclinical Alzheimer's disease.

For biochemical analysis we used fresh-frozen occipital and temporal lobe tissue from 10 patients with Alzheimer's disease, 20 patients with pathologically preclinical Alzheimer's disease and 10 control subjects (Table 2).

The human brain tissue used in this study originated from the Brain Bank of the Laboratory of Neuropathology at the University of Ulm (Germany). This brain bank collects brain tissue in accordance with German legal regulations. The project was approved by the ethics committee of the University of Ulm.

Immunohistochemistry

Morphological and immunohistochemical analyses were carried out on cases shown in Table 1 and 2 ($n = 73$; Case B25 was not included because only frozen tissue was available). Paraffin sections from the human medial lobe and the occipital cortex were stained with anti-$A\beta_{17-24}$, anti-$A\beta_{42}$, anti-$A\beta_{N3pE}$, and anti-phosphorylated Aβ (Kim *et al.*, 1988; Saido *et al.*, 1995; Yamaguchi *et al.*, 1998; Kumar *et al.*, 2011) (Supplementary Table 1). The primary antibodies were detected with biotinylated anti-mouse and anti-rabbit IgG secondary antibodies and visualized with avidin-biotin-complex (ABC-Kit, Vector Laboratories) and diaminobenzidine-HCl (DAB). The sections were counterstained with haematoxylin. Positive and negative controls were performed.

Double-label immunofluorescence was performed to demonstrate colocalization of Aβ with $A\beta_{N3pE}$ and phosphorylated Aβ in a given plaque. Anti-$A\beta_{17-24}$ and anti-$A\beta_{N3pE}$, anti-$A\beta_{42}$ (IBL, polyclonal) (Supplementary Table 1) and anti-phosphorylated Aβ (monoclonal) as well as anti-$A\beta_{N3pE}$ and anti-phosphorylated Aβ (monoclonal) were combined. Polyclonal rabbit antibodies were detected with Cy2 or Cy3-labelled secondary antibodies against rabbit IgG. Likewise, monoclonal mouse antibodies were visualized with Cy2 or Cy3-labelled secondary antibodies against mouse IgG (Dianova).

Quantification of amyloid-β load

Aβ load was determined as the percentage of the area in the temporal neocortex (Brodmann area 36) covered by Aβ plaques detected with anti-$A\beta_{17-24}$. Morphometry for Aβ load determination was performed using ImageJ image processing and analysis software (National Institutes of Health). For plaque measurements the area of the morphologically identified plaques was interactively delineated with a cursor and then measured by using the ImageJ software package (National Institutes of Health). The areas of all plaques in a given cortical region were added up. The area of the respective cortex areas was likewise measured by interactive delineation with a cursor. Accordingly, the $A\beta_{N3pE}$ load was determined as the percentage of the temporal neocortex area covered by anti-$A\beta_{N3pE}$-positive plaques and the phosphorylated Aβ load by that of anti-phosphorylated Aβ-positive plaques.

Preparation of native human brain lysates

Biochemical analysis was carried out from cases shown in Table 2. Protein extraction from fresh frozen brain (0.04 g) was carried out in 2 ml Tris-buffered saline containing a protease and phosphatase inhibitor-cocktail (Complete and PhosSTOP, Roche). The tissue was homogenized with Micropestle (Eppendorf) before sonication. The homogenate was centrifuged for 30 min at 14 000*g* at 4°C. The supernatant with the soluble and dispersible fraction not separated from one another was retained. The pellet containing the membrane-associated and the solid plaque-associated fraction was resuspended in 2% SDS (Fig. 1). Ultracentrifugation of the supernatant at 175 000*g* was used to separate the soluble, i.e. the supernatant after ultracentrifugation, from the dispersible fraction, i.e. the resulting pellet (Fig. 1). The pellet of the dispersible fraction was resuspended in TBS and stored at −80°C until further use. After separation from the soluble and the dispersible fraction, the SDS-resuspended pellet was centrifuged at 14 000*g*, and the supernatant was kept as membrane-associated SDS fraction (Fig. 1). The pellet was further dissolved in 70% formic acid and the homogenate was lyophilized by centrifuging in the vacuum centrifuge (Vacufuge; Eppendorf) and reconstituted in 100 µl of 2× lithium dodecyl sulphate sample buffer (Invitrogen) before heating at 70°C for 5 min. The resulting sample was considered as plaque-associated, formic acid-soluble fraction (Mc Donald *et al.*, 2010). The total protein amounts of soluble, dispersible, and membrane-associated fractions were determined using BCA Protein Assay (Bio-Rad).

Immunoprecipitation

For immunoprecipitation, 200 µl of the native soluble and dispersible fractions from the brain lysates were incubated with 1 µl A11 antibodies against non-fibrillar oligomers, B10AP antibody fragments for precipitation of protofibrils and fibrils, anti-$A\beta_{N3pE}$ or anti-phosphorylated Aβ at 4°C for 4 h as previously described (Rijal Upadhaya *et al.*, 2012*a*) (Supplementary Table 1). Protein G Microbeads (50 µl; Miltenyi Biotec) were added to the mixture and incubated overnight at 4°C. The mixture was then passed through the µ Columns which separate the microbeads by retaining them in the column, while the rest of the lysate flows through. After one mild washing step with TBS at pH 7.4 the microbead-bound proteins were eluted with 95°C heated lithium dodecyl sulphate sample buffer (Invitrogen). To verify specific precipitation of non-fibrillar oligomers with A11 and protofibrils and fibrils with B10AP and to exclude contamination with membrane-coated microsomes, precipitates were analysed for non-fibrillar oligomeric or protofibrillar/fibrillar protein structure by transmission electron microscopy as previously published (Rijal Upadhaya *et al.*, 2012*b*).

Western blot analysis

The four fractions (soluble, dispersible, membrane-associated and plaque-associated) as well as immunoprecipitation eluates were analysed by SDS-PAGE and subsequent western blot analysis with anti-$A\beta_{1-17}$, anti-phosphorylated Aβ and anti-$A\beta_{N3pE}$ antibodies (Supplementary Table 1). $A\beta_{40}$ and $A\beta_{42}$ were detected with C-terminus specific antibodies (Supplementary Table 1) after precipitation of $A\beta_{N3pE}$ and phosphorylated Aβ to clarify whether these post-translational modifications occur in both Aβ peptides, $A\beta_{40}$ and $A\beta_{42}$. Blots were developed with an ECL detection system (Supersignal Pico Western system, ThermoScientific-Pierce) and illuminated in ECL Hyperfilm (GE Healthcare).

Because Aβ aggregates readily dissociate in the presence of SDS-containing buffers into monomers and small oligomers, such as dimers, trimers, or Aβ*56 (Rijal Upadhaya *et al.*, 2012*b*; Watt *et al.*, 2013), we analysed differences among the monomer bands that indicate changes in the protein levels of precipitated Aβ aggregates densitometrically using ImageJ software (National Institutes of Health).

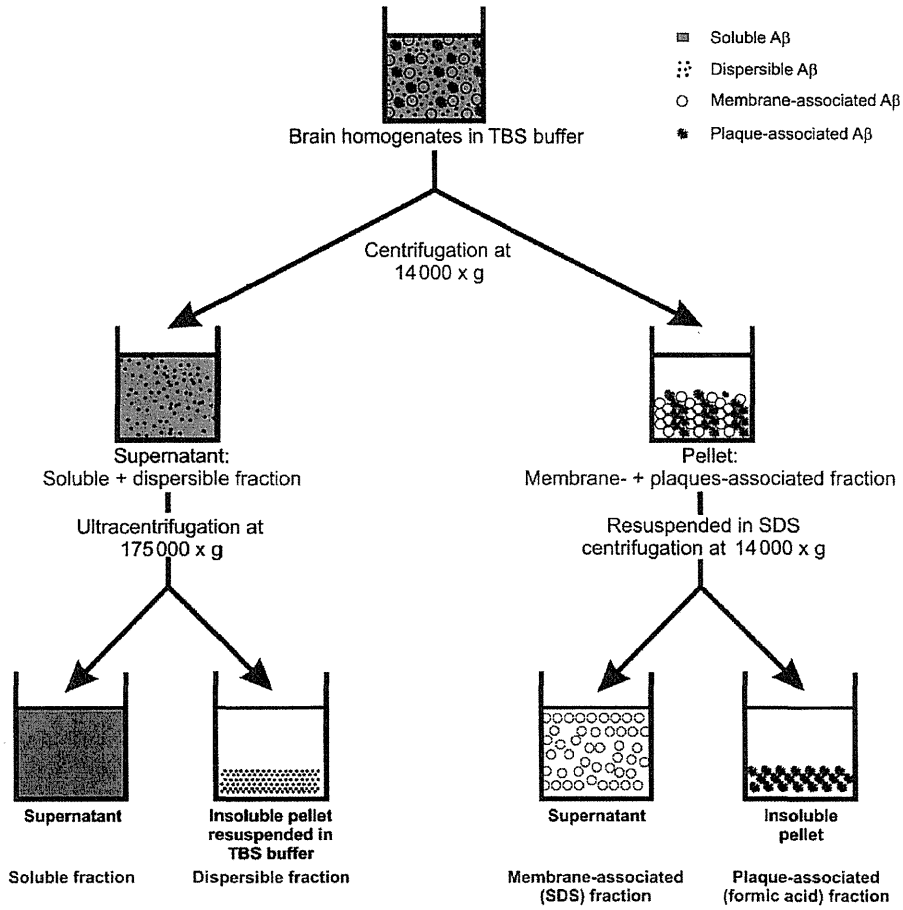

Figure 1 Schematic representation of the biochemical fractionation of brain tissue homogenates into soluble, dispersible, membrane-associated SDS-soluble, and plaque-associated (formic acid-soluble) fraction. The dispersible fraction also contains microsomes. Isolation of dispersible oligomers, protofibrils, and fibrils by immunoprecipitation with oligomer or protofibril/fibril-specific antibodies is necessary as previously shown (Rijal Upadhaya *et al.*, 2012*a*, *b*).

This method allows a semi-quantitative assessment of Aβ as previously described in detail (Rijal Upadhaya *et al.*, 2012*a*).

Statistical analysis

SPSS-Statistics 19.0 (SPSS) software was used to calculate statistical tests. One-way ANOVA was used to compare densitometric data received from western blot quantification and Aβ loads among cases with Alzheimer's disease, pathologically preclinical Alzheimer's disease and control cases. The Games-Howell *post hoc* test was used to correct for multiple testing. Binary logistic regression analysis controlled for age and gender was used to test whether dementia was associated with Aβ, $Aβ_{N3pE}$, and phosphorylated Aβ loads. Partial correlation analysis was performed for Aβ–medial temporal lobe phase, Braak–neurofibrillary tangle stage, CERAD score for neuritic plaques, and the biochemical stages of Aβ aggregation and accumulation (biochemical–Aβ stages) as determined in this study. Likewise, partial correlation analysis controlled for age and gender was also carried out among Aβ–medial temporal lobe phase, Braak–neurofibrillary tangle stage, CERAD score for neuritic plaques, and a modified biochemical-Aβ stage represented by the detection of Aβ, $Aβ_{N3pE}$, and phosphorylated Aβ in plaques. Fisher's exact test with subsequent trend test was performed to clarify whether the biochemical-Aβ stages and biochemical-Aβ stage analogues for plaques increase hierarchically with progression of the clinical stage of Alzheimer's disease from non-Alzheimer's disease to pathologically preclinical Alzheimer's disease and finally to symptomatic Alzheimer's disease.

Results

Biochemical detection of soluble, dispersible, membrane-associated and plaque-associated amyloid-β

SDS-PAGE and western blot analysis with anti-$Aβ_{1–17}$ demonstrated Aβ in the soluble, dispersible, membrane-associated and plaque-associated fraction in neocortex homogenates from cases

with Alzheimer's disease and cases with pathologically preclinical Alzheimer's disease. As previously shown Aβ dimers, trimers etc. represent SDS treatment-related dissociation products of larger Aβ aggregates (Rijal Upadhaya *et al.*, 2012*b*; Watt *et al.*, 2013). Therefore, we did not consider them for a separate analysis in this study. The semi-quantitative assessment of the monomer band density has been demonstrated previously to correlate with the amount of Aβ aggregates (Rijal Upadhaya *et al.*, 2012*a*) and was used for the semi-quantitative assessment of Aβ aggregates in a given biochemical fraction or being precipitated with A11 and B10AP. Control cases showed no detectable Aβ (Fig. 2A and Supplementary Fig. 1A). Semi-quantitatively, cases with Alzheimer's disease exhibited significantly more Aβ-positive material than cases with pathologically preclinical Alzheimer's disease and non-Alzheimer's disease control cases in all fractions. Pathologically preclinical Alzheimer's disease cases showed more Aβ-positive material than non-Alzheimer's disease controls (Fig. 2A and Supplementary Table 2A).

$A\beta_{N3pE}$ was observed in the soluble, dispersible, membrane-associated and plaque-associated fraction of symptomatic Alzheimer's disease brain homogenates. Cases with pathologically preclinical Alzheimer's disease exhibited no or only small amounts of soluble and dispersible $A\beta_{N3pE}$. SDS-soluble $A\beta_{N3pE}$ in the membrane-associated fraction and/or plaque-associated $A\beta_{N3pE}$ was detected in 13 of 20 cases with pathologically preclinical Alzheimer's disease by western blotting. Some cases with pathologically preclinical Alzheimer's disease, thereby, exhibited similar amounts of SDS-soluble $A\beta_{N3pE}$ as symptomatic cases with Alzheimer's disease (Fig. 2B and Supplementary Fig. 1B). Semi-quantitative comparison of monomer bands from control, pathologically preclinical Alzheimer's disease and Alzheimer's disease cases revealed that Alzheimer's disease cases exhibited significantly more $A\beta_{N3pE}$ in all four fractions than controls and cases with pathologically preclinical Alzheimer's disease. No significant differences in the levels of soluble and plaque-associated Aβ were observed between control and pathologically preclinical Alzheimer's disease cases whereas such differences were seen in the dispersible and membrane-associated fraction (Fig. 2B and Supplementary Table 2A).

Phosphorylated Aβ was found in the dispersible, membrane-associated; and plaque-associated fraction of Alzheimer's disease brain homogenates. Soluble phosphorylated Aβ was not observed. Cases with pathologically preclinical Alzheimer's disease did not exhibit detectable levels of phosphorylated Aβ in the membrane-associated and plaque-associated fractions. Only isolated pathologically preclinical Alzheimer's disease cases showed few phosphorylated Aβ in the dispersible fraction. Phosphorylated Aβ was not detected in control cases. A second ~8 kDa band was also detected with the phosphorylated Aβ antibody. This band presented with similar intensity in soluble, dispersible, and membrane-associated fractions of Alzheimer's disease, pathologically preclinical Alzheimer's disease, and control cases as well as in ischiadic nerve samples (Supplementary Fig. 3). Therefore, we did not interpret this band as a dimer-specific band but as unspecific co-staining without any relevance for Alzheimer's disease because a similar ~8 kDa band was not observed in the formic acid-soluble, plaque-associated fraction although dimers were seen (Fig. 2C and Supplementary Fig. 1C). Significant differences in the semi-quantitative assessment of the phosphorylated Aβ monomer bands detected by western blotting were not observed (Fig. 2C and Supplementary Table 2A).

To clarify whether the occurrence of $A\beta_{N3pE}$ and phosphorylated Aβ in Alzheimer's disease and pathologically preclinical Alzheimer's disease cases was related to a specific accumulation in Aβ oligomers, protofibrils, and/or fibrils we performed immunoprecipitation and western blotting. Non-fibrillar oligomers were precipitated from soluble and dispersible fractions with A11 antibodies whereas protofibrils and fibrils were precipitated with B10AP antibody fragments. These precipitates contained Aβ aggregates as well as oligomeric, protofibrillar, or fibrillar aggregates composed of other proteins (Rijal Upadhaya *et al.*, 2012*b*). The highest amounts of oligomeric and protofibrillar/fibrillar Aβ aggregates were found in precipitates of the dispersible fraction of Alzheimer's disease cases. Cases with pathologically preclinical Alzheimer's disease had detectable but lower levels of dispersible Aβ oligomers, protofibrils, and fibrils than Alzheimer's disease cases. Non-Alzheimer's disease controls did not contain measurable amounts of Aβ. The amounts of soluble Aβ oligomers, protofibrils, and fibrils did not vary significantly between Alzheimer's disease and pathologically preclinical Alzheimer's disease but were higher in cases with Alzheimer's disease and cases with pathologically preclinical Alzheimer's disease than in controls (Fig. 3A, Supplementary Fig. 2A and Supplementary Table 2B).

$A\beta_{N3pE}$ was not detected in soluble oligomers, protofibrils, and fibrils precipitated with A11 and B10AP but in dispersible oligomers, protofibrils, and fibrils of Alzheimer's disease and pathologically preclinical Alzheimer's disease cases. Non-Alzheimer's disease controls did not display such material. Although dispersible $A\beta_{N3pE}$ oligomers, protofibrils, and fibrils appeared to occur in higher levels in Alzheimer's disease neocortex than in pathologically preclinical Alzheimer's disease these differences were not significant (Fig. 3B, Supplementary Fig. 2B and Supplementary Table 2C).

Dispersible phosphorylated Aβ-containing oligomers, protofibrils, and fibrils were found in higher amounts in Alzheimer's disease cases compared to non-Alzheimer's disease controls and pathologically preclinical Alzheimer's disease cases. The amount of dispersible phosphorylated Aβ oligomers, protofibrils and fibrils did not vary significantly between non-Alzheimer's disease controls and pathologically preclinical Alzheimer's disease cases. Only a few pathologically preclinical Alzheimer's disease cases exhibited small amounts of phosphorylated Aβ-containing protofibrils. Soluble phosphorylated Aβ in precipitated oligomers, protofibrils and fibrils was not observed. An 8-kDa band stained with anti-phosphorylated Aβ was considered unspecific and not relevant for Alzheimer's disease because it was seen in similar intensity in non-Alzheimer's disease controls, pathologically preclinical Alzheimer's disease, symptomatic Alzheimer's disease cases (Fig. 3C, Supplementary Fig. 2C and Supplementary Table 2C) and in western blots of peripheral nervous tissue of the ischiadic nerve (Supplementary Fig. 3). The fact that it was observed after immunoprecipitation with A11 and B10AP indicates a cross-reaction with components of non-Aβ protein complexes sharing A11 and B10AP conformation specific epitopes.

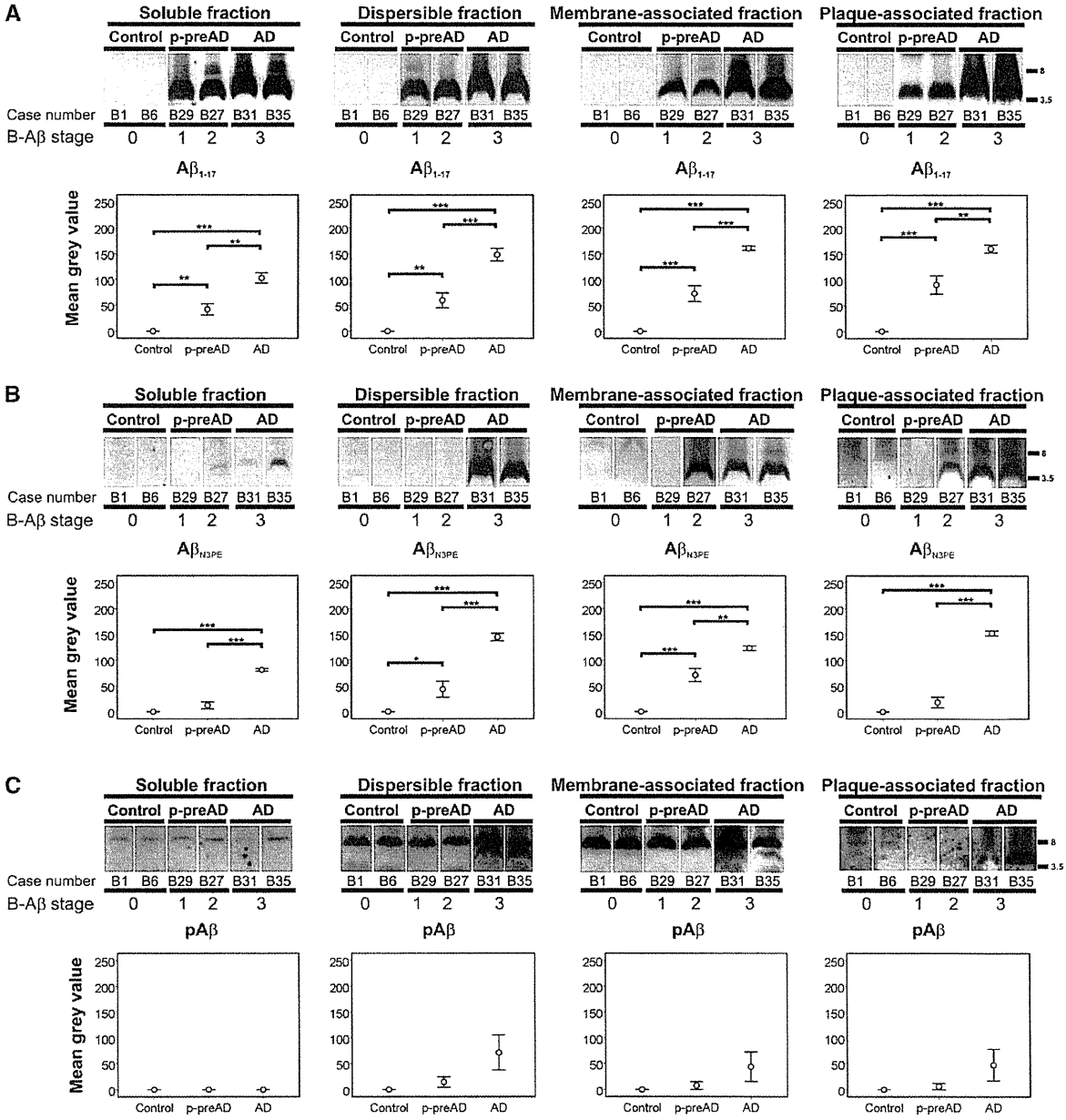

Figure 2 Biochemical detection of soluble, dispersible, membrane-associated and plaque-associated Aβ. (**A**) Denaturing SDS-PAGE analysis of soluble, dispersible, membrane-associated (SDS-soluble) and plaque-associated (formic acid-soluble) fractions of human brain homogenates. Aβ was detected with anti-$Aβ_{1-17}$. Quantification revealed highest levels of soluble, dispersible, membrane-associated, and plaque-associated Aβ in Alzheimer's disease cases whereas pathologically preclinical Alzheimer's disease cases (p-preAD) exhibited lower Aβ levels than Alzheimer's disease cases but higher levels than non-Alzheimer's disease controls, which lack detectable amounts of Aβ aggregates. (**B**) Cases with symptomatic Alzheimer's disease exhibited higher levels of soluble, dispersible, membrane-associated and plaque-associated (formic acid soluble) $Aβ_{N3pE}$ than pathologically preclinical Alzheimer's disease and control cases. Significant differences occurred between pathologically preclinical Alzheimer's disease and control cases only in the dispersible and membrane-associated fraction. Soluble, dispersible and plaque-associated $Aβ_{N3pE}$ was nearly absent in pathologically preclinical Alzheimer's disease cases. SDS-soluble membrane-associated and plaque-associated $Aβ_{N3pE}$ was observed in some pathologically preclinical Alzheimer's disease cases whereas other pathologically preclinical Alzheimer's disease cases did not exhibit $Aβ_{N3pE}$ distinguishing biochemical-Aβ stages 1 and 2. An additional dimer band was visible in the plaque-associated fraction. (**C**) Phosphorylated Aβ was not found in the soluble fraction. In the dispersible, membrane-associated and plaque-associated fractions phosphorylated Aβ monomer bands (4 kDa) were visible in cases with Alzheimer's disease exhibiting biochemical-Aβ stage 3 whereas most pathologically preclinical Alzheimer's disease cases did not exhibit phosphorylated Aβ monomer bands. No significant quantitative differences were observed after western blot analysis. The 8 kDa band stained with anti-phosphorylated Aβ was considered unspecific and not relevant for Alzheimer's disease because it was seen in

(continued)

In summary, human Alzheimer's disease brains can be distinguished from non-Alzheimer's disease and pathologically preclinical Alzheimer's disease brains by increasing amounts of soluble and dispersible Aβ oligomers, protofibrils, and fibrils whereby phosphorylation of Aβ at serine 8 was associated with dispersible Aβ oligomers, protofibrils, and fibrils in the Alzheimer's disease neocortex. The biochemical composition of Aβ aggregates showed a hierarchical sequence in which Aβ, $Aβ_{N3pE}$, and phosphorylated Aβ occurred in dispersible, membrane-associated and plaque-associated Aβ-aggregates. All 10 cases with Alzheimer's disease and 14 of 20 cases with pathologically preclinical Alzheimer's disease exhibited biochemically detectable Aβ. Six cases with pathologically preclinical Alzheimer's disease and the 10 non-Alzheimer's disease cases did not show biochemically detectable amounts of Aβ (Fig. 2A and 3A). Twelve pathologically preclinical Alzheimer's disease and all 10 Alzheimer's disease cases also showed anti-$Aβ_{N3pE}$-positive material in the Aβ aggregates, suggesting a second stage in the development of Aβ aggregation. Phosphorylated Aβ was found only in 4 of 20 cases with pathologically preclinical Alzheimer's disease, but in all 10 Alzheimer's disease cases studied biochemically in a presumably third stage of this process. These three stages of the biochemical aggregation and accumulation are referred to here as biochemical-Aβ stages 1–3.

Immunoprecipitation of post-translational modified $Aβ_{N3pE}$ and phosphorylated Aβ with subsequent detection of the $Aβ_{40}$ and $Aβ_{42}$ C-terminus with C-terminus specific antibodies revealed that $Aβ_{N3pE-40}$, $Aβ_{N3pE-42}$, phosphorylated $Aβ_{40}$, and phosphorylated $Aβ_{42}$ can be detected in the human Alzheimer's disease and pathologically preclinical Alzheimer's disease cortex with stronger signals for the $Aβ_{42}$-C-terminus peptides (Supplementary Fig. 4A).

Immunohistochemical detection of amyloid-β, $Aβ_{N3pE}$ and phosphorylated amyloid-β in senile plaques

Immunohistochemical staining of brain tissues from all Alzheimer's disease and pathologically preclinical Alzheimer's disease cases exhibited Aβ plaques detectable with antibodies raised against $Aβ_{17–24}$ and $Aβ_{42}$. All cases with Alzheimer's disease and 30 of 33 pathologically preclinical Alzheimer's disease cases also showed immunopositivity for anti-$Aβ_{N3pE}$. Eleven of the pathologically preclinical Alzheimer's disease cases with anti-$Aβ_{N3pE}$ positive plaques and all Alzheimer's disease cases also had phosphorylated Aβ positive plaques. This hierarchical sequence of plaque staining with anti-$Aβ_{17–24}$, anti-$Aβ_{N3pE}$, and anti-phosphorylated Aβ was identical with that seen for the biochemical detection of Aβ and its accumulation in the dispersible, membrane-associated and plaque-associated fractions of brain homogenates. This sequence of plaque staining is referred to as biochemical-Aβ stage analogue for plaques. However, 6 of 20 cases with pathologically preclinical Alzheimer's disease cases with $Aβ_{17–24}$-positive plaques (Table 2) did not exhibit significant amounts of biochemically detectable Aβ. In two further cases with $Aβ_{N3pE}$-positive plaques Aβ was seen biochemically but no $Aβ_{N3pE}$. Four of 16 cases with phosphorylated Aβ-positive plaques did not exhibit phosphorylated Aβ in the western blot and immunoprecipitation analysis.

Aβ plaques detected with antibodies raised against $Aβ_{17–24}$ and $Aβ_{42}$ were prevalent in all pathologically preclinical Alzheimer's disease and Alzheimer's disease cases (Fig. 4A–C). Alzheimer's disease cases exhibited higher Aβ loads than pathologically preclinical Alzheimer's disease cases. Non-Alzheimer's disease controls had lower Aβ loads than in Alzheimer's disease and pathologically preclinical Alzheimer's disease cases (Fig. 5A and Supplementary Table 2D).

$Aβ_{N3pE}$ positive plaques were frequently observed in most pathologically preclinical Alzheimer's disease cases and in all Alzheimer's disease cases (Fig. 4D–F). All types of plaques exhibited $Aβ_{N3pE}$. $Aβ_{N3pE}$ plaque loads were lower than total $Aβ_{1–40/42}$ plaque loads. Alzheimer's disease cases had higher $Aβ_{N3pE}$ plaque loads than cases with pathologically preclinical Alzheimer's disease. Cases with pathologically preclinical Alzheimer's disease exhibited higher $Aβ_{N3pE}$ plaque loads than non-Alzheimer's disease controls (Fig. 5A and B and Supplementary Table 2D).

The phosphorylated Aβ plaque loads were lower than the Aβ and $Aβ_{N3pE}$ plaque loads. However, in Alzheimer's disease cases the phosphorylated Aβ plaque load was higher than in pathologically preclinical Alzheimer's disease. Non-Alzheimer's disease controls exhibited no anti-phosphorylated Aβ-positive plaques whereas some cases with pathologically preclinical Alzheimer's disease showed few phosphorylated Aβ-positive plaques. The phosphorylated Aβ plaque load in pathologically preclinical Alzheimer's disease cases was slightly higher than in control cases (Figs 4G, H and 5C and Supplementary Table 2D). Single pathologically preclinical Alzheimer's disease cases exhibiting high amounts of $Aβ_{17–24}$ and $Aβ_{N3pE}$-positive plaques did not exhibit phosphorylated Aβ within these plaques in consecutive sections (Supplementary Fig. 5).

Logistic regression analysis controlled for age and gender revealed a significant association of the Aβ load, $Aβ_{N3pE}$ load and the phosphorylated Aβ load with Alzheimer's disease cases in comparison to cases with pathologically preclinical Alzheimer's disease and non-Alzheimer's disease control cases ($P < 0.05$; detailed statistical analysis see Supplementary Table 2E).

Double-label immunohistochemistry revealed that in Alzheimer's disease cases most Aβ plaques also exhibit $Aβ_{N3pE}$ whereas phosphorylated Aβ was usually restricted to a subset of plaques, especially cored plaques (Supplementary Fig. 4B–J).

Figure 2 Continued

non-Alzheimer's disease controls, pathologically preclinical Alzheimer's disease and symptomatic Alzheimer's disease cases in similar intensity. Case numbers according to Supplementary Table 1B are provided. Statistical analysis was performed by ANOVA with Games-Howell *post hoc* test: $*P < 0.05$; $**P < 0.01$; $***P < 0.001$ (Alzheimer's disease, $n = 10$; pathologically preclinical Alzheimer's disease, $n = 20$; control, $n = 10$; Supplementary Table 2A–C). AD = Alzheimer's disease; B-Aβ-stage = biochemical-Aβ stage; pAβ = phosphorylated Aβ; p-preAD = pathologically (diagnosed) Alzheimer's disease.

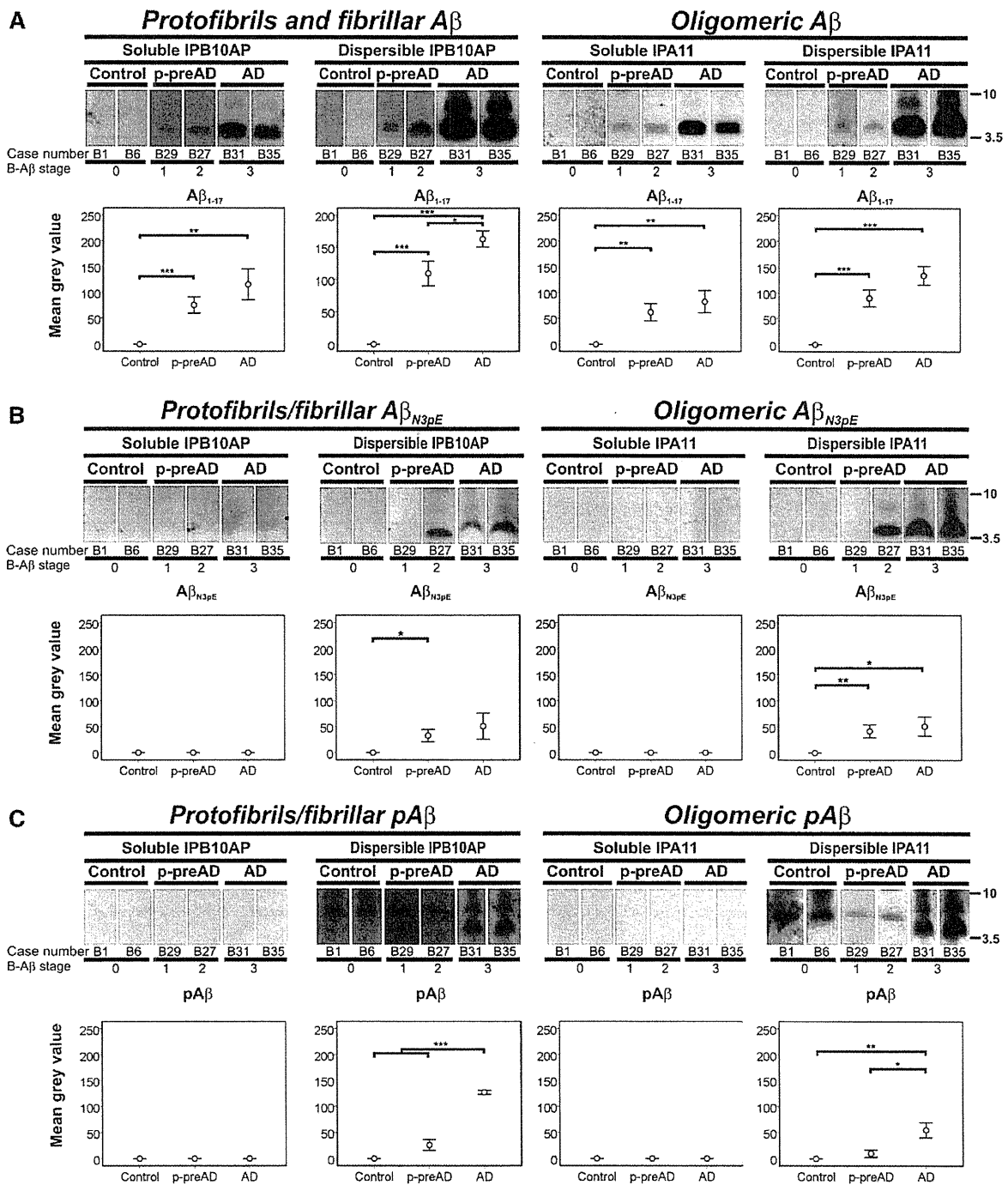

Figure 3 (**A**) Analysis of B10AP immunoprecipitated protofibrils and fibrils and A11 immunoprecipitated non-fibrillar oligomers revealed highest levels of these in the soluble and dispersible fractions of Alzheimer's disease cases. Pathologically preclinical Alzheimer's disease cases exhibited fewer Aβ oligomers, protofibrils, and fibrils than Alzheimer's disease cases but more than non-Alzheimer's disease controls, which did not show Aβ oligomers, protofibrils or fibrils. (**B**) In the precipitated protofibrils, fibrils, and oligomers, $Aβ_{N3pE}$ was found only in the dispersible but not in the soluble fraction. The levels of $Aβ_{N3pE}$ oligomers, protofibrils and fibrils were not significantly different between Alzheimer's disease and pathologically preclinical Alzheimer's disease cases but higher than in non-Alzheimer's disease controls. Only a subset of pathologically preclinical Alzheimer's disease cases (p-preAD) exhibited $Aβ_{N3pE}$ indicative of biochemical-Aβ stage 2 whereas other pathologically preclinical Alzheimer's disease cases with anti-$Aβ_{1-17}$ positive Aβ aggregates did not exhibit anti-$Aβ_{N3pE}$-positive material representing biochemical-Aβ stage 1. (**C**) Dispersible phosphorylated Aβ oligomers, protofibrils, and fibrils were nearly restricted to Alzheimer's disease cases whereas non-Alzheimer's disease controls and pathologically preclinical Alzheimer's disease exhibited nearly negligible amounts. Phosphorylated Aβ in patients with Alzeimer's disease represented the third stage of the biochemical development of Aβ aggregates

(continued)

Correlations between the biochemical stages of amyloid-β aggregation and accumulation with the hallmark lesions of Alzheimer's disease and its associations with dementia

The biochemical-Aβ stages correlated with the Aβ–medial temporal lobe phase ($r = 0.79$, $P < 0.001$), the Braak–neurofibrillary tangle-stage ($r = 0.609$, $P = 0.001$), and the CERAD score for neuritic plaques ($r = 0.56$, $P = 0.002$) as well as with the overall NIA-AA degree of Alzheimer's disease pathology ($r = 0.683$, $P < 0.001$; detailed statistical analysis is shown in Supplementary Table 2F).

Likewise, the biochemical-Aβ stage analogue for plaques correlated with the Aβ–medial temporal lobe-phase ($r = 0.834$, $P < 0.001$), the Braak–neurofibrillary tangle-stage ($r = 0.564$, $P = 0.002$), the CERAD score for neuritic plaques ($r = 0.429$, $P = 0.023$), the overall NIA-AA degree of Alzheimer's disease pathology ($r = 0.76$, $P < 0.001$; detailed statistical analysis is shown in Supplementary Table 2G) as well as with the biochemical-Aβ stages ($r = 0.688$, $P < 0.001$).

Using Fisher's exact test with a subsequent trend test there was a significant association between the increasing clinical stage of Alzheimer's disease from non-Alzheimer's disease to pathologically preclinical Alzheimer's disease and finally to symptomatic Alzheimer's disease with the biochemical-Aβ stage and the biochemical-Aβ stage analogue for plaques ($P < 0.001$; detailed statistical analysis Supplementary Table 2H).

Discussion

The major findings of this study are: (i) the prevalence of $Aβ_{N3pE}$ and phosphorylated Aβ in dispersible, membrane-associated, and plaque-associated Aβ aggregates showed a hierarchical sequence of three stages, in which these post-translationally modified Aβ species occurred in Aβ aggregates: biochemical-Aβ stage 1 = aggregation of $Aβ_{1–40/42}$ alone, biochemical-Aβ stage 2 = additional detection of $Aβ_{N3pE}$, and biochemical-Aβ stage 3 = aggregation of $Aβ_{1–40/42}$, $Aβ_{N3pE–40/42}$, and phosphorylated $Aβ_{40/42}$ (Fig. 6); (ii) the phosphorylation of Aβ at serine 8 and its aggregation in dispersible oligomers, protofibrils and fibrils was associated with symptomatic Alzheimer's disease but not with pathologically preclinical Alzheimer's disease and controls; (iii) the amounts of soluble and dispersible Aβ oligomers, protofibrils and fibrils increased with the development from non-Alzheimer's disease to pathologically preclinical Alzheimer's disease and then to Alzheimer's disease; and (iv) $Aβ_{N3pE}$ and phosphorylated Aβ were not detectable in soluble oligomers, protofibrils and fibrils but in dispersible ones.

Dispersible, membrane-associated, and plaque-associated Aβ aggregates exhibited a hierarchical sequence, in which $Aβ_{1-40/42}$, $Aβ_{N3pE}$, and phosphorylated Aβ occurred in these aggregates. This sequence allowed the distinction of three biochemical stages of Aβ aggregation and accumulation (biochemical-Aβ stages). The first stage was characterized by the detection of $Aβ_{1–40/42}$ in the absence of detectable amounts of $Aβ_{N3pE}$ and phosphorylated Aβ. Biochemical-Aβ stage 2 was characterized by the additional occurrence of $Aβ_{N3pE}$-positive material in these aggregates in the absence of phosphorylated Aβ. Phosphorylated Aβ in biochemical-Aβ stage 3 was restricted to those cases that already exhibited anti-Aβ and anti-$Aβ_{N3pE}$-positive material. $Aβ_{N3pE–40}$, $Aβ_{N3pE–42}$, phosphorylated $Aβ_{40}$, and phosphorylated $Aβ_{42}$ were all found in cases with Alzheimer's disease with biochemical-Aβ-stage 3. However, $Aβ_{N3pE-42}$ and phosphorylated $Aβ_{42}$ were the predominant forms. This sequence was further confirmed by the finding of a similar hierarchical sequence in the occurrence of Aβ, $Aβ_{N3pE}$, and phosphorylated Aβ in senile plaques in controls, cases with pathologically preclinical Alzheimer's disease, and cases with symptomatic Alzheimer's disease. Comparison between biochemical detection of Aβ aggregates and immunohistochemistry revealed that the biochemical detection of Aβ aggregates by western blotting was less sensitive than immunostaining for plaques. A possible explanation for this finding is that those cases with initial plaque deposition have only very few plaques that may not be included in the samples taken for biochemical analysis or that the amount of plaque-pathology is too low for detection in brain homogenates. The hierarchical staining pattern of plaques and Aβ aggregates seen in this study can be explained by either a hierarchical occurrence of these Aβ species in the aggregates or by different sensitivities of the antibodies. Arguments in favour of a hierarchical occurrence of $Aβ_{1–40/42}$, $Aβ_{N3pE}$ and phosphorylated Aβ are that the antibody sensitivity of anti-$Aβ_{N3pE}$ and anti-phosphorylated Aβ were quite similar (Saido *et al.*, 1995; Kumar *et al.*, 2013) and did not explain the differences between biochemical-Aβ stages 2 and 3, and that biochemical-Aβ stage 1 cases already exhibited significant anti-$Aβ_{1–17}$ positive material in the absence of $Aβ_{N3pE}$ and phosphorylated Aβ signals. Moreover, this sequence was seen in Aβ aggregates in brain homogenates as well as in plaques stained immunohistochemically with these antibodies. A further argument in favour of a hierarchical sequence in which Aβ aggregates accumulate distinct types of Aβ peptides is provided by previous reports showing that Aβ plaques first stain for $Aβ_{42}$, second for $Aβ_{40}$ (Iwatsubo *et al.*, 1996; Lemere *et al.*, 1996) followed by $Aβ_{N3pE}$ (Iwatsubo *et al.*, 1996), then for $Aβ_{N11pE}$, and, finally, in very few cases, for $Aβ_{17-40/42}$ (P3) (Iwatsubo *et al.*, 1996;

Figure 3 Continued

throughout the pathogenesis of Alzheimer's disease (biochemical-Aβ stage 3). The 8 kDa band stained with anti-phosphorylated Aβ was considered unspecific and not relevant for Alzheimer's disease because it was seen in non-Alzheimer's disease controls, pathologically preclinical Alzheimer's disease and symptomatic Alzheimer's disease cases in similar intensity. No phosphorylated Aβ containing oligomers, protofibrils and fibrils were found in the soluble fraction. Case numbers according to Supplementary Table 1B are provided. Statistical analysis was performed by ANOVA with Games-Howell *post hoc* test: $*P < 0.05$; $**P < 0.01$; $***P < 0.001$ (Alzheimer's disease, $n = 10$; pathologically preclinical Alzheimer's disease, $n = 20$; control, $n = 10$; Supplementary Table 2A–C). AD = Alzheimer's disease; B-Aβ-stage = biochemical-Aβ stage; pAβ = phosphorylated Aβ; p-preAD = pathologically (diagnosed) Alzheimer's disease.

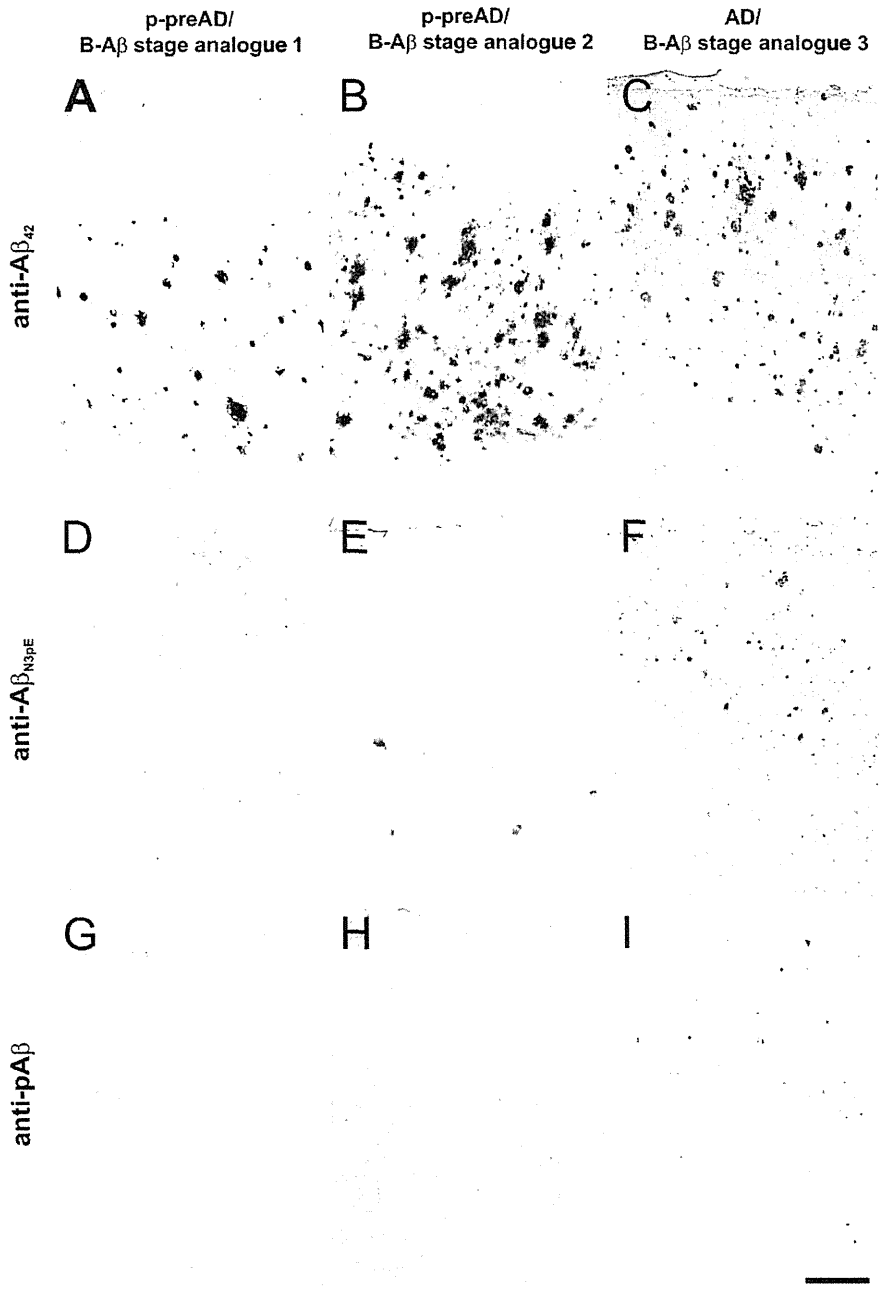

Figure 4 (**A–C**) Aβ plaques detected with anti-$Aβ_{42}$ were found in both Alzheimer's disease and pathologically preclinical Alzheimer's disease cases. The biochemical-Aβ stage analogues for plaques were provided. (**D–F**) $Aβ_{N3pE}$ was found in pathologically preclinical Alzheimer's disease cases of biochemical-Aβ stage analogue 2 and in Alzheimer's disease cases. In the biochemical-Aβ stage analogue 1 case depicted in **D** no anti-$Aβ_{N3pE}$-positive plaques were found. (**G–I**) Phosphorylated Aβ was absent in biochemical-Aβ stage analogues 1 and 2 pathologically preclinical Alzheimer's disease cases (**G** and **H**) but prevalent in the biochemical-Aβ stage 3 case with Alzheimer's disease (**I**). Calibration bar in **H** corresponds to 400 μm (valid for **A–I**). **A**, **D** and **G**: Case A15; **B**, **E** and **H**: Case A14; **C**, **F** and **I**: Case A30. AD = Alzheimer's disease; B-Aβ-stage analog = biochemical-Aβ stage analogue; pAβ = phosphorylated Aβ; p-preAD = pathologically (diagnosed) Alzheimer's disease.

Thal *et al.*, 2005). As $Aβ_{40}$ and $Aβ_{42}$ both occur very early in the development of Aβ plaque pathology and as $Aβ_{N11pE}$ was seen in plaques of Alzheimer's disease as well as of pathologically preclinical Alzheimer's disease cases, we focused our study on Aβ, $Aβ_{N3pE}$ and phosphorylated Aβ. These three different Aβ peptides exhibited a robust hierarchical sequence that provides a backbone for the determination of other peptides and their relation to the development of Alzheimer's disease-related Aβ aggregation.

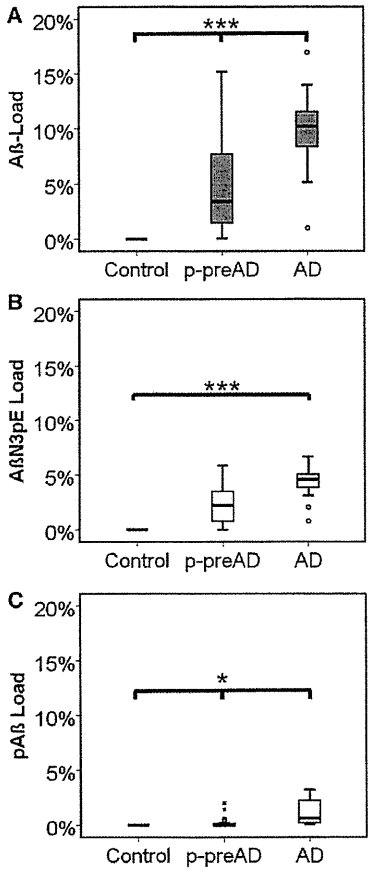

Figure 5 Aβ load, $Aβ_{N3pE}$ load, and phosphorylated Aβ load in Alzheimer's disease, pathologically preclinical Alzheimer's disease (p-preAD) and control cases. (**A**) The Aβ load increased gradually from control to pathologically preclinical Alzheimer's disease and then to Alzheimer's disease cases. (**B**) The $Aβ_{N3pE}$ load in pathologically preclinical Alzheimer's disease and Alzheimer's disease cases was higher than in non-Alzheimer's disease cases. Significant differences in the $Aβ_{N3pE}$ load between pathologically preclinical Alzheimer's disease and Alzheimer's disease cases were not observed. (**C**) Alzheimer's disease cases had significantly higher phosphorylated Aβ loads compared with control and pathologically preclinical Alzheimer's disease cases. ANOVA with Games-Howell *post hoc* test: $*P < 0.05$; $***P < 0.001$ (Supplementary Table 2E). AD = Alzheimer's disease; pAβ = phosphorylated Aβ; p-preAD = pathologically (diagnosed) Alzheimer's disease.

A limitation of autopsy studies is that only a single time point can be analysed for each individual. To minimize this limitation we used the Aβ phase, the Braak–neurofibrillary tangle stage, and the CERAD score for neuritic plaque pathology as widely accepted pathological markers for Alzheimer's disease progression (Hyman *et al.*, 2012). The biochemical-Aβ stages, thereby, correlated with the phases of Aβ plaque distribution (Thal *et al.*, 2002), the Braak–neurofibrillary tangle stages for neurofibrillary tangle distribution (Braak and Braak, 1991) and with the CERAD score for neuritic plaque pathology (Mirra *et al.*, 1991). This correlation was not simply an effect of ageing because we used partial correlation analysis controlled for age and gender, a statistical method that allows one to calculate the correlation between two parameters independent from age and gender effects. Interestingly, the occurrence and amount of phosphorylated Aβ in biochemical-Aβ stage 3 cases was associated with symptomatic Alzheimer's disease but not with pathologically preclinical Alzheimer's disease. As such, it is tempting to speculate that the biochemical composition of Aβ aggregates changes with the progression of Alzheimer's disease from pathologically preclinical Alzheimer's disease to Alzheimer's disease cases. Hence, we assume that cases with Alzheimer's disease contain more soluble and dispersible Aβ oligomers, protofibrils, and fibrils than pathologically preclinical Alzheimer's disease and non-Alzheimer's disease cases and the presence of modified $Aβ_{N3pE}$ and phosphorylated Aβ peptides may stabilize dispersible oligomeric, protofibrillar and fibrillar Aβ aggregates. An argument in favour of this hypothesis is that both $Aβ_{N3pE}$ and phosphorylated Aβ have the ability to stabilize Aβ aggregates (Schlenzig *et al.*, 2009; Kumar *et al.*, 2011). An alternative explanation for the increased amounts of $Aβ_{N3pE}$ and phosphorylated Aβ in Alzheimer's disease cases in comparison with pathologically preclinical Alzheimer's disease cases is that both are by-products of an increased production or decreased clearance of Aβ without relevance for the disease and its progression. Accordingly, the accumulation of such by-products would be expected to be more predominant in symptomatic Alzheimer's disease cases compared with pathologically preclinical Alzheimer's disease cases, and $Aβ_{N3pE}$ and phosphorylated Aβ would accumulate in parallel with Aβ plaques detected with anti-$Aβ_{17-24}$ or anti-$Aβ_{42}$. However, this was not the case for phosphorylated Aβ. As depicted in Supplementary Fig. 5 isolated pathologically preclinical Alzheimer's disease cases exhibited very high amounts of $Aβ_{17-24}$ and $Aβ_{N3pE}$-positive plaques, even more than some Alzheimer's disease cases, but no phosphorylated Aβ. On the other hand, phosphorylated Aβ was seen in all symptomatic Alzheimer's disease cases, even in those that had fewer plaques than some pathologically preclinical Alzheimer's disease cases. Another argument against the hypothesis that $Aβ_{N3pE}$ and phosphorylated Aβ are by-products of Aβ accumulation without specific impact on the disease is that both modified forms of Aβ are more prone to form oligomeric and fibrillar aggregates *in vitro* than non-modified Aβ (Saido *et al.*, 1995; Schlenzig *et al.*, 2009; Kumar *et al.*, 2011). As such, $Aβ_{N3pE}$ and phosphorylated Aβ promote the formation of oligomeric, protofibrillar and fibrillar aggregates of Aβ and the biochemical-Aβ stages more likely document the biochemical development of Aβ aggregates in the pathogenesis of Alzheimer's disease. For all that, it is not yet clear whether $Aβ_{N3pE}$ and phosphorylated Aβ play a directing role in the pathogenesis of Alzheimer's disease. At least, they serve as marker proteins for the progression of the disease as shown here.

It is important to note that the biochemical development of Aβ aggregates starts with the aggregation of Aβ in all four fractions received after brain homogenization. Immunoprecipitation with B10AP antibody fragments and A11 revealed that these initial Aβ aggregates already contain Aβ oligomers, protofibrils and fibrils. Given the sequence of events in the biochemical-Aβ stages, it is tempting to speculate that modification of initial Aβ aggregates by adding detectable amounts of $Aβ_{N3pE}$ and phosphorylated Aβ

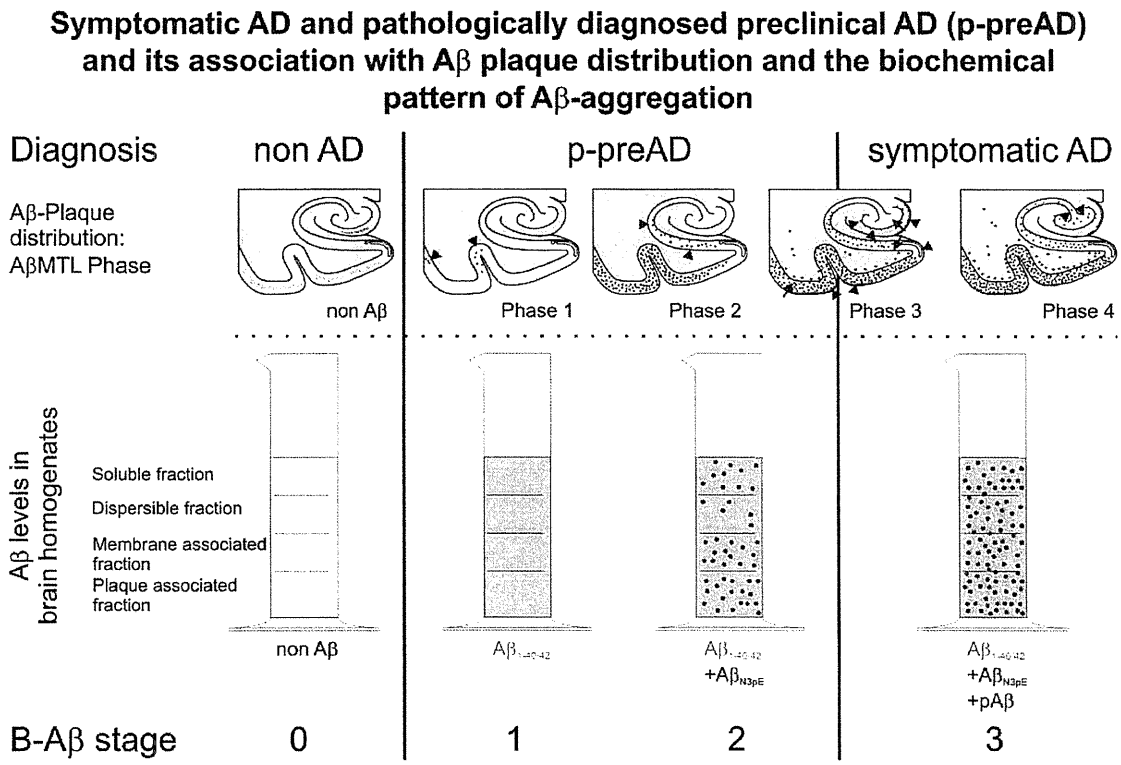

Figure 6 Associations between the diagnosis of Alzheimer's disease, pathologically preclinical Alzheimer's disease and control cases with the biochemical-Aβ stages of the biochemical composition of Aβ aggregates and with the Aβ-medial temporal lobe phases. 'Non-Alzheimer's disease' is by definition the absence of Aβ plaques. Pathologically preclinical Alzheimer's disease cases and cases with symptomatic Alzheimer's disease can be distinguished by the distribution of Aβ plaque pathology in the brain as represented in the medial temporal lobe (Thal *et al.*, 2000, 2002, 2013) but also by changes in the biochemical composition of soluble, dispersible, membrane-associated, and plaque-associated Aβ aggregates as represented by the biochemical-Aβ stages. These differences in the biochemical composition of Aβ aggregates between cases with pathologically preclinical Alzheimer's disease and Alzheimer's disease cases are indicated by the detection of phosphorylated Aβ in symptomatic Alzheimer's disease cases and by the detection of $Aβ_{N3pE}$ in the soluble and dispersible fraction. The hierarchical sequence, in which $Aβ_{1–40/42}$, $Aβ_{N3pE}$, and phosphorylated Aβ occurred in the Aβ aggregates in the human brain, thereby, allowed the distinction of three biochemical-Aβ stages: biochemical-Aβ stage 1 was defined by the detection of anti-Aβ-positive Aβ aggregates in the absence of detectable amounts of $Aβ_{N3pE}$ and phosphorylated Aβ; biochemical-Aβ stage 2 was characterized by additional $Aβ_{N3pE}$ in the aggregates without detectable phosphorylated Aβ; biochemical-Aβ stage 3 represented Aβ aggregates in the brain exhibiting all three types of Aβ, i.e. $Aβ_{1–40/42}$, $Aβ_{N3pE}$, and phosphorylated Aβ. AD = Alzheimer's disease; AβMTL phase = Aβ medial temporal lobe phase; B-Aβ-stage = biochemical-Aβ stage; pAβ = phosphorylated Aβ; p-preAD = pathologically (diagnosed) Alzheimer's disease.

peptides to these aggregates is a critical event for the development of Alzheimer's disease. Phosphorylation of Aβ at serine 8 indicating biochemical-Aβ stage 3 rather than the mere presence of $Aβ_{N3pE}$, thereby seems to be critical for conversion from pathologically preclinical Alzheimer's disease to Alzheimer's disease. Arguments in favour of this hypothesis are: (i) pathologically preclinical Alzheimer's disease cases do not exhibit significant amounts of phosphorylated Aβ in dispersible oligomers, protofibrils and fibrils but Alzheimer's disease cases do; (ii) cases with Alzheimer's disease have significant numbers of phosphorylated Aβ-containing plaques (phosphorylated Aβ plaque load = 1.21%) whereas the phosphorylated Aβ plaque load was in mean <0.28% in pathologically preclinical Alzheimer's disease cases; and (iii) $Aβ_{N3pE}$ is already present in significant amounts in plaques ($Aβ_{N3pE}$ plaque load = 2.25%), dispersible oligomers, protofibrils, fibrils, and in the SDS-soluble membrane-associated fraction in pathologically preclinical Alzheimer's disease cases and increases quantitatively in Alzheimer's disease ($Aβ_{N3pE}$ plaque load = 4.22%) but does not indicate a qualitative change in the composition of Aβ aggregates between Alzheimer's disease and pathologically preclinical Alzheimer's disease cases because $Aβ_{N3pE}$ already occurs in biochemical-Aβ stage 2, which is seen in pathologically preclinical Alzheimer's disease cases, and in biochemical-Aβ stage 3 in Alzheimer's disease cases. In the event that phosphorylation of Aβ increases its tendency to form dispersible aggregates and, thereby, supports conversion from pathologically preclinical Alzheimer's disease to Alzheimer's disease, blocking or modulation of Aβ phosphorylation would be an appropriate mechanism to prevent or delay the conversion from pathologically preclinical Alzheimer's disease to symptomatic Alzheimer's disease. An aggregation promoting the role for phosphorylated Aβ has been demonstrated (Kumar *et al.*, 2011). However, it is important to

test this potential treatment strategy in an appropriate animal model to exclude the possibility that phosphorylated Aβ is merely a by-product of the disease without therapeutic potential.

Phosphorylation of serine residues by protein kinase A similar to serine 8 of the Aβ peptide (Kumar *et al.*, 2011) is also seen in tau protein (Andorfer and Davies, 2000). Thus, one could assume that Aβ and tau phosphorylation are two results of a common problem: increased phosphorylation of proteins in the Alzheimer's disease brain. Arguments against this hypothesis are that: (i) dispersible Aβ alone was associated with neurodegeneration in APP transgenic mice with an increased Aβ production (Rijal Upadhaya *et al.*, 2012*a*); (ii) Aβ was capable of exacerbating tau pathology in tau transgenic mice (Gotz *et al.*, 2001; Lewis *et al.*, 2001) suggesting a causative or at least triggering role for Aβ in Alzheimer's disease-related neurodegeneration; and (iii) tau phosphorylation occurs early in the pathogenesis of neuronal alterations in Alzheimer's disease (Braak *et al.*, 2011) as well as in other non-Alzheimer's disease tauopathies (Dickson *et al.*, 2011), whereas Aβ phosphorylation at serine 8 is a late event mainly restricted to symptomatic Alzheimer's disease cases, as shown here.

As $Aβ_{N3pE}$ and phosphorylated Aβ have also been found in APP/PS1 transgenic mice without inducing significant levels of tau pathology the hierarchical accumulation of different forms of Aβ peptides alone may not cause Alzheimer's disease, but in the presence of mild, pre-existing tau pathology as it is regularly the case in elderly humans (Braak *et al.*, 2011), Aβ aggregates may exacerbate tau pathology as also seen in mouse models for Alzheimer's disease (Gotz *et al.*, 2001; Lewis *et al.*, 2001; Oddo *et al.*, 2004).

Our finding, that soluble and dispersible Aβ oligomers, protofibrils and fibrils increase from pathologically preclinical Alzheimer's disease to Alzheimer's disease cases is in line with the previously reported detection of Aβ oligomers, protofibrils and fibrils in Alzheimer's disease cases (Kayed *et al.*, 2003; Habicht *et al.*, 2007; Mc Donald *et al.*, 2010). However, our data apparently contradict reports by other authors showing that the Aβ plaque loads did not vary significantly between Alzheimer's disease and non-demented cases with plaque pathology (Arriagada *et al.*, 1992*b*) and that increasing cognitive decline in patients with Alzeimer's disease could not be explained by differences in the Aβ loads (Arriagada *et al.*, 1992*a*). Of note, in the present study, some pathologically preclinical Alzheimer's disease cases had higher amyloid plaque loads in the temporal neocortex than some cases with Alzheimer's disease (Supplementary Fig. 5). This might explain the lack of statistically significant differences in Aβ loads reported in the abovementioned studies. However, when staining Aβ plaques for phosphorylated Aβ we found significant differences between pathologically preclinical Alzheimer's disease and Alzheimer's disease cases in the respective phosphorylated Aβ plaque loads indicating that changes in the biochemical composition of the Aβ aggregates occur when pathologically preclinical Alzheimer's disease cases convert to symptomatic Alzheimer's disease, i.e. the conversion from biochemical-Aβ stage 2 to biochemical-Aβ stage 3. These qualitative changes were also found biochemically in dispersible Aβ oligomers, protofibrils, and fibrils as well as in the membrane-associated and plaque-associated fractions.

Although it is tempting to assume that the hierarchical sequences of Aβ plaque distribution and that of the biochemical evolution of Alzheimer's disease-related Aβ aggregates represent a pathogenetic sequence of events it is possible that this sequence can be held at a given point or that Aβ deposition is even reversible until a given point in this sequence. Accordingly, cases classified as pathologically preclinical Alzheimer's disease (non-demented individuals with Alzheimer's disease pathology according to current NIA-AA criteria for the neuropathological diagnosis of Alzheimer's disease (Hyman *et al.*, 2012)) do not necessarily develop symptomatic Alzheimer's disease.

The non-Alzheimer's disease control and pathologically preclinical Alzheimer's disease cases included in this study were identified at autopsy and were not tested for Alzheimer's disease biomarkers, such as CSF-Aβ and CSF-tau protein or amyloid PET. Therefore, the pathologically preclinical Alzheimer's disease cases in our study cannot be compared with clinically detectable preclinical Alzheimer's disease cases according to Vos *et al.* (2013). However, it will be an important issue for future research to verify the neuropathological and biochemical correlatives in amyloid PET-positive or CSF-biomarker positive non-demented cases and to distinguish them from cases with symptomatic Alzheimer's disease and non-Alzheimer's disease.

The missing signals for $Aβ_{N3pE}$ and phosphorylated Aβ in the soluble oligomers, protofibrils, and fibrils argue in favour of aggregation promoting effects of both post-translational modified Aβ species as previously described *in vitro* (Schlenzig *et al.*, 2009; Kumar *et al.*, 2011). However, $Aβ_{N3pE}$ was observed in the soluble fraction of Alzheimer's disease cases indicating that presumably smaller $Aβ_{N3pE}$ oligomers are present in the Alzheimer's disease brain that cannot be precipitated with A11 and B10AP.

In conclusion, we have shown qualitative differences in the composition of Aβ plaques and dispersible Aβ oligomers, protofibrils and fibrils between Alzheimer's disease and pathologically preclinical Alzheimer's disease cases that allow the distinction of three biochemical-Aβ stages. Although it appears quite obvious that non-phosphorylated full-length Aβ accumulates before truncated and phosphorylated forms become detectable, their sequence of occurrence was associated with a critical step in the pathogenesis of Alzheimer's disease: phosphorylated Aβ, indicative for biochemical-Aβ stage 3, was specifically associated with symptomatic Alzheimer's disease. Thus, phosphorylated Aβ may support further accumulation of Aβ oligomers, protofibrils, and fibrils in the event that pathologically preclinical Alzheimer's disease converts into Alzheimer's disease. Phosphorylation of Aβ at serine 8 may be a new therapeutic target to prevent conversion from pathologically preclinical Alzheimer's disease to Alzheimer's disease.

Acknowledgements

The authors thank Professor Johannes Attems and Dr. Kelly Del Tredici for his/her helpful comments on this manuscript.

Funding

This study was supported by DFG-grants WA1477/6-2 (J.W.), TH624/4-2, TH624/6-1, Alzheimer Forschung Initiative Grants #10810, #13803 (D.R.T.), #12854 (S.K.), SFB610 and the Landesexzellenz-Netzwerk "Biowissenschaften" (Sachsen-Anhalt) (M.F.).

Conflict of interest

D.R.T. received consultant honorary from Simon-Kucher and Partners (Germany), and GE-Healthcare (UK) and collaborated with Novartis Pharma Basel (Switzerland). C.A.F.v.A. received honoraria from serving on the scientific advisory board of Nutricia GmbH and has received funding for travel and speaker honoraria from Sanofi-Aventis, Novartis, Pfizer, Eisai and Nutricia GmbH, and received research support from Heel GmbH.

Supplementary material

Supplementary material is available at *Brain* online.

References

Alafuzoff I, Arzberger T, Al-Sarraj S, Bodi I, Bogdanovic N, Braak H, et al. Staging of neurofibrillary pathology in Alzheimer's disease. A study of the BrainNet Europe Consortium. Brain Pathol 2008; 18: 484–96.

Alzheimer A. Ueber eine eigenartige Erkrankung der Hirnrinde. Allg Zschr Psych 1907; 64: 146–8.

Andorfer CA, Davies P. PKA phosphorylations on tau: developmental studies in the mouse. Dev Neurosci 2000; 22: 303–9.

Arriagada PV, Growdon JH, Hedley-Whyte ET, Hyman BT. Neurofibrillary tangles but not senile plaques parallel duration and severity of Alzheimer's disease. Neurology 1992a; 42: 631–9.

Arriagada PV, Marzloff K, Hyman BT. Distribution of Alzheimer-type pathologic changes in nondemented elderly individuals matches the pattern in Alzheimer's disease. Neurology 1992b; 42: 1681–8.

Braak H, Alafuzoff I, Arzberger T, Kretzschmar H, Del Tredici K. Staging of Alzheimer disease-associated neurofibrillary pathology using paraffin sections and immunocytochemistry. Acta Neuropathol 2006; 112: 389–404.

Braak H, Braak E. Neuropathological stageing of Alzheimer-related changes. Acta Neuropathol 1991; 82: 239–59.

Braak H, Thal DR, Ghebremedhin E, Del Tredici K. Stages of the pathological process in Alzheimer's disease: age categories 1 year to 100 years. J Neuropathol Exp Neurol 2011; 70: 960–9.

Dickson DW, Kouri N, Murray ME, Josephs KA. Neuropathology of frontotemporal lobar degeneration-tau (FTLD-tau). J Mol Neurosci 2011; 45: 384–9.

Dubois B, Feldman HH, Jacova C, Dekosky ST, Barberger-Gateau P, Cummings J, et al. Research criteria for the diagnosis of Alzheimer's disease: revising the NINCDS-ADRDA criteria. Lancet Neurol 2007; 6: 734–46.

Gotz J, Chen F, van Dorpe J, Nitsch RM. Formation of neurofibrillary tangles in P301l tau transgenic mice induced by Abeta 42 fibrils. Science 2001; 293: 1491–5.

Habicht G, Haupt C, Friedrich RP, Hortschansky P, Sachse C, Meinhardt J, et al. Directed selection of a conformational antibody domain that prevents mature amyloid fibril formation by stabilizing Abeta protofibrils. Proc Natl Acad Sci USA 2007; 104: 19232–7.

Harper JD, Wong SS, Lieber CM, Lansbury PT. Observation of metastable Abeta amyloid protofibrils by atomic force microscopy. Chem Biol 1997; 4: 119–25.

Hyman BT, Phelps CH, Beach TG, Bigio EH, Cairns NJ, Carrillo MC, et al. National Institute on Aging–Alzheimer's Association guidelines for the neuropathologic assessment of Alzheimer's disease. Alzheimers Dement 2012; 8: 1–13.

Iwatsubo T, Saido TC, Mann DM, Lee VM, Trojanowski JQ. Full-length amyloid-beta (1-42(43)) and amino-terminally modified and truncated amyloid-beta 42(43) deposit in diffuse plaques. Am J Pathol 1996; 149: 1823–30.

Kayed R, Head E, Thompson JL, McIntire TM, Milton SC, Cotman CW, et al. Common structure of soluble amyloid oligomers implies common mechanism of pathogenesis. Science 2003; 300: 486–9.

Kim KS, Miller DL, Sapienza VJ, Chen C-MJ, Bai C, Grundke-Iqbal I, et al. Production and characterization of monoclonal antibodies reactive to synthetic cerebrovascular amyloid peptide. Neurosci Res Commun 1988; 2: 121–30.

Kumar S, Rezaei-Ghaleh N, Terwel D, Thal DR, Richard M, Hoch M, et al. Extracellular phosphorylation of the amyloid beta-peptide promotes formation of toxic aggregates during the pathogenesis of Alzheimer's disease. EMBO J 2011; 30: 2255–65.

Kumar S, Wirths O, Theil S, Gerth J, Bayer TA, Walter J. Early intraneuronal accumulation and increased aggregation of phosphorylated Abeta in a mouse model of Alzheimer's disease. Acta Neuropathol 2013; 125: 699–709.

Lemere CA, Blusztajn JK, Yamaguchi H, Wisniewski T, Saido TC, Selkoe DJ. Sequence of deposition of heterogeneous amyloid beta-peptides and APO E in Down syndrome: implications for initial events in amyloid plaque formation. Neurobiol Dis 1996; 3: 16–32.

Lesne S, Koh MT, Kotilinek L, Kayed R, Glabe CG, Yang A, et al. A specific amyloid-beta protein assembly in the brain impairs memory. Nature 2006; 440: 352–7.

Lewis J, Dickson DW, Lin WL, Chisholm L, Corral A, Jones G, et al. Enhanced neurofibrillary degeneration in transgenic mice expressing mutant tau and APP. Science 2001; 293: 1487–91.

Masters CL, Multhaup G, Simms G, Pottgiesser J, Martins RN, Beyreuther K. Neuronal origin of a cerebral amyloid: neurofibrillary tangles of Alzheimer's disease contain the same protein as the amyloid of plaque cores and blood vessels. EMBO J 1985; 4: 2757–63.

Mc Donald JM, Savva GM, Brayne C, Welzel AT, Forster G, Shankar GM, et al. The presence of sodium dodecyl sulphate-stable Abeta dimers is strongly associated with Alzheimer-type dementia. Brain 2010; 133: 1328–41.

Mirra SS, Heyman A, McKeel D, Sumi SM, Crain BJ, Brownlee LM, et al. The Consortium to Establish a Registry for Alzheimer's Disease (CERAD). Part II. Standardization of the neuropathologic assessment of Alzheimer's disease. Neurology 1991; 41: 479–86.

Monsell SE, Mock C, Roe CM, Ghoshal N, Morris JC, Cairns NJ, et al. Comparison of symptomatic and asymptomatic persons with Alzheimer disease neuropathology. Neurology 2013; 80: 2121–9.

Morris JC. The Clinical Dementia Rating (CDR): current version and scoring rules. Neurology 1993; 43: 2412–4.

Morris JC, Heyman A, Mohs RC, Hughes JP, van Belle G, Fillenbaum G, et al. The Consortium to Establish a Registry for Alzheimer's Disease (CERAD). Part I. Clinical and neuropsychological assessment of Alzheimer's disease. Neurology 1989; 39: 1159–65.

Oddo S, Billings L, Kesslak JP, Cribbs DH, LaFerla FM. Abeta immunotherapy leads to clearance of early, but not late, hyperphosphorylated tau aggregates via the proteasome. Neuron 2004; 43: 321–32.

Rijal Upadhaya A, Capetillo-Zarate E, Kosterin I, Abramowski D, Kumar S, Yamaguchi H, et al. Dispersible amyloid β-protein oligomers, protofibrils, and fibrils represent diffusible but not soluble aggregates: their role in neurodegeneration in amyloid precursor protein (APP) transgenic mice. Neurobiol Aging 2012a; 33: 2641–60.

Rijal Upadhaya A, Lungrin I, Yamaguchi H, Fändrich M, Thal DR. High-molecular weight Aβ-oligomers and protofibrils are the predominant

Aβ-species in the native soluble protein fraction of the AD brain. J Cell Mol Med 2012b; 16: 287–95.

Saido TC, Iwatsubo T, Mann DM, Shimada H, Ihara Y, Kawashima S. Dominant and differential deposition of distinct beta-amyloid peptide species, A beta N3(pE), in senile plaques. Neuron 1995; 14: 457–66.

Schlenzig D, Manhart S, Cinar Y, Kleinschmidt M, Hause G, Willbold D, et al. Pyroglutamate formation influences solubility and amyloidogenicity of amyloid peptides. Biochemistry 2009; 48: 7072–8.

Shankar GM, Li S, Mehta TH, Garcia-Munoz A, Shepardson NE, Smith I, et al. Amyloid-beta protein dimers isolated directly from Alzheimer's brains impair synaptic plasticity and memory. Nat Med 2008; 14: 837–42.

Sperling RA, Aisen PS, Beckett LA, Bennett DA, Craft S, Fagan AM, et al. Toward defining the preclinical stages of Alzheimer's disease: recommendations from the National Institute on Aging-Alzheimer's Association workgroups on diagnostic guidelines for Alzheimer's disease. Alzheimers Dement 2011; 7: 280–92.

Thal DR, Capetillo-Zarate E, Schultz C, Rüb U, Saido TC, Yamaguchi H, et al. Apolipoprotein E co-localizes with newly formed amyloid beta-protein (Abeta)-deposits lacking immunoreactivity against N-terminal epitopes of Abeta in a genotype-dependent manner. Acta Neuropathol 2005; 110: 459–71.

Thal DR, Rüb U, Orantes M, Braak H. Phases of Abeta-deposition in the human brain and its relevance for the development of AD. Neurology 2002; 58: 1791–800.

Thal DR, Rüb U, Schultz C, Sassin I, Ghebremedhin E, Del Tredici K, et al. Sequence of Abeta-protein deposition in the human medial temporal lobe. J Neuropathol Exp Neurol 2000; 59: 733–48.

Thal DR, von Arnim C, Griffin WS, Yamaguchi H, Mrak RE, Attems J, et al. Pathology of clinical and preclinical Alzheimer's disease. Eur Arch Psychiatry Clin Neurosci 2013; 263(Suppl 2): S137–45.

Vos SJ, Xiong C, Visser PJ, Jasielec MS, Hassenstab J, Grant EA, et al. Preclinical Alzheimer's disease and its outcome: a longitudinal cohort study. Lancet Neurol 2013; 12: 957–65.

Walsh DM, Lomakin A, Benedek GB, Condron MM, Teplow DB. Amyloid beta-protein fibrillogenesis. Detection of a protofibrillar intermediate. J Biol Chem 1997; 272: 22364–72.

Watt AD, Perez KA, Rembach A, Sherrat NA, Hung LW, Johanssen T, et al. Oligomers, fact or artefact? SDS-PAGE induces dimerization of beta-amyloid in human brain samples. Acta Neuropathol 2013; 125: 549–64.

Yamaguchi H, Sugihara S, Ogawa A, Saido TC, Ihara Y. Diffuse plaques associated with astroglial amyloid beta protein, possibly showing a disappearing stage of senile plaques. Acta Neuropathol 1998; 95: 217–22.

原著

群馬県の認知症疾患医療センターの活動実績と受診経過

山口　晴保[1)]，中島　智子[2)]，内田　成香[2)]，野中　和英[2)]
松本　美江[2)]，牧　　陽子[1)]，山口　智晴[1)]，高玉　真光[2)]

要　旨

【目的】群馬県の認知症疾患医療センター（認セ）の活動状況を示す．【方法】群馬県10認セの活動状況のデータ分析と，1地域型認セ（当認セ）の経過観察63例での分析を行った．【結果】1）県全体では相談者6,000名/年，鑑別診断数3,000名/年で実績が伸びている．2）当認セは，相談者が100名/月，鑑別診断数が60名/月と，地域型としては高い活動であった．神経内科・老年科主体で運営している認セの方が，精神科主体よりも相談者数と鑑別診断数が約2倍高かった．3）当認セ診療継続54例で，3か月後にMMSEの有意な上昇と，行動障害尺度DBD高値群での有意な低下を認めた．【まとめ】群馬県は概ね二次医療圏域ごとに地域型認セを配置して，「認知症の人の在宅生活を支える」というオレンジプランの趣旨に沿った活動ができている．

キーワード：認知症疾患医療センター，認知症，地域連携，オレンジプラン

1．はじめに

2012年度から施行された改正介護保険法の理念は「地域包括ケアシステムの構築」であり，認知症の人が日常生活圏域の中で必要なサービスを受けて生活し続けることを支援するために，認知症サポート医養成研修事業，かかりつけ医認知症対応力向上研修事業，認知症疾患医療センター（認セ）運営事業などの認知症施策が行われている（武田，堀部，2012）．2013年6月に発表された「認知症施策推進5か年計画（オレンジプラン）」では，病院・施設への長期入院・入所を避けて『在宅生活を継続させる方向性』がより明確に示された（厚生労働省ホームページ，2012）．

認セの整備事業は，2008年度予算に新規事業1.9億円（1/2国庫補助事業；自治体負担と合わせて3.8億円）として盛り込まれてスタートした．「認知症疾患医療センター運用事業実施要綱」では，その役割を1）専門医療相談，2）鑑別診断とそれに基づく初期対応，3）合併症・周辺症状への急性期対応，4）かかりつけ医等への研修会の開催，5）認知症疾患医療連携協議会の開催，6）情報発信と定めた（そ

Medical Centers for Dementia in Gunma: their activities and follow-up data

Haruyasu Yamaguchi[1)], Tomoko Nakajima[2)], Haruka Uchida[2)], Kazuhide Nonaka[2)], Mie Matsumoto[2)], Yohko Maki[1)], Tomoharu Yamaguchi[1)], Masamitsu Takatama[2)]

[1)] 群馬大学大学院保健学研究科［〒371-8514　前橋市昭和町3-39-22］
Gunma University Graduate School of Health Sciences (3-39-22 Showacho Maebashi, 371-8514, Japan)

[2)] 老年病研究所附属病院認知症疾患医療センター［〒371-0847 前橋市大友町3-26-8］
Geriatrics Research Institute and Hospital (3-26-8 Otomocho, Maebashi, 371-0847, Japan)

の後，基幹型では7）救急・急性期対応（空床確保）が加わった）．熊本県は2009年に大学病院の認セを中心にして各医療圏域に認セを配置する，いわゆる熊本方式で設置を行った（小嶋，池田，2012）．これを受けて，2010年から厚生労働省は，全ての機能を持つ基幹型と，救急・急性期対応の空床確保機能を持たない地域型の指定を行うようになった．その後，予算規模も拡大し，2013年12月20日には全47都道府県と17政令指定都市で総数250か所（基幹型12か所，地域型238か所）が指定された（2014年1月10日厚生労働省問い合わせ）．今後，オレンジプラン（2013年～2017年度の5年間）では，二次医療圏に地域型を1か所以上，センター機能を補完する「認知症医療支援診療所（仮称）」を含めて全国で500か所の設置をめざしている（厚生労働省ホームページ，2012）．

熊本県は，厚生労働省の指針では県内に2か所のセンターが設置される予算規模であった．しかし，県内全域の支援態勢を作るために，基幹型センター1か所（熊本大学；池田学センター長）と7か所（その後2か所追加）の地域に密着した地域拠点型センターを2009年に設置し，8（10）か所のセンターが一丸となって認知症医療に取り組むという，斬新なシステムを構築した．これが「熊本方式」である．

群馬県においては，2009年に，2か所の精神科病院を認セに指定する方向という新聞報道があった．そこで，筆者は，「熊本方式」を県の担当者に提言した．また，認セ設置要綱では精神科病院ではなく総合病院を指定することが基本になっていることも指摘した．そして，群馬県では，精神科病院という限定を外して公募が行われ，群馬大学が中核型，他に地域型6か所という熊本方式の配置で，2010年9月に認セがスタートした．2011年2月に地域型3か所が追加指定されて全10か所（10二次医療圏域中の8圏域に配置）となり，2011年4月からは主管が県庁障害政策課から介護高齢課に移った．群馬県では，基幹型の指定条件である救急・急性期対応の空床確保を満たさない群馬大学附属病院を，群馬県独自の「中核型」，他の9施設を地域型として指定した．地域型9病院のうち6病院と多くは精神科中心で，残り3病院は神経内科・老人科中心に運営されている．

本報告では，群馬県全体の認セの活動状況を報告すると共に，老年病研究所附属病院認セの特性と，受診継続して3か月後に再評価できた症例について，認知機能や行動障害などについての経過を報告する．

2. 対象と方法

2.1. 群馬県全体の認知症疾患医療センターのデータ

群馬県の認セ10か所の活動状況のデータは，群馬県介護高齢課の担当者より得た．これを分析し，図表化した．認セの認定は2010年9月に始まり2011年2月に県内10か所態勢が整ったが，県への実績報告が新書式となった2011年4月からのデータを分析した．

2.2. 老年病研究所附属認知症疾患医療センター（当認セ）

当認セ受診者の基本データを分析し，図表化した．また，当認セを鑑別診断目的に受診した後も，当センターでフォローできたケースのうち，2012年7月～2013年3月までに初診し，3か月後の2013年6月までに再診した63例を対象に経過を分析した．追跡指標は，認知機能はmini-mental state examination（MMSE），行動障害はdementia behavior disturbance scale（DBD），介護負担はZarit介護負担尺度8項目日本語版（Zarit-8）とした．統計はStatcel2（OMS出版）を用いた．

同伴者の属性についても分析した．複数の同伴者がいる場合は，DBDなどの質問紙に回答した者を同伴者とした．

当認セのデータを分析するに当たり，公益財団法人老年病研究所倫理委員会の審査を受けて承認を得た（第24号）．

なお，当認セには1名の臨床心理士と1名の精神保健福祉士が専従で，加えて精神保健福祉士や社会福祉士，認知症認定看護師，作業療法士などが専任，兼任や非常勤で関わって協力している．医師は，非

常勤を含めて5名の神経内科医と1名の内科医が中心になって外来診療を行っている.

3. 結　果

3.1. 群馬県の認知症疾患医療センターの状況

全10か所の相談延べ件数，相談者数（相談者の実数），鑑別診断数，入院者数の月間合計数の推移をFig. 1に示した．なお，受診者数の集計は，一部の施設が延べ件数（再診も含めた件数）で県に報告していたために，信頼性の点から図には含めていない．この問題は2013年4月からは是正されている．

2011年4月からの6か月と直近の6か月（2013年10月まで）を年間数に換算して比較してみると，群馬県全体の相談延べ件数は，当初の4,000件/年から8,000件/年，相談者数は当初の約3,000名/年から直近の約6,000名/年に倍増している．過去1年の相談延べ件数（実数）は，1認セ当たり平均770件/年，中央値591件/年で，レンジは314～1,213件/年であった．相談者数は，1認セ当たり平均559名/年，中央値523名/年で，レンジは252～1,013名/年で認セ間に約4倍の開きがあった．相談者数を運営主体別にみると，神経内科・老年科が主体の認セでは平均744名/年（レンジ：252～1,013名/年），精神科主体の6認セでは437名/年（264～706名/年）と神経内科・老年科主体の認セが約1.8倍の数値となった。

鑑別診断数は，群馬県全体で当初の約1,800名/年から直近の約3,000名/年と，発足から2年ほどで，実績は1.7倍に増えた．2013年10月までの1年間の鑑別診断実数は，1認セ当たり平均285名/年，中央値250名/年で，レンジは81～625名/年と認セ間で8倍近い大きな開きがあった．鑑別診断数を運営主体別にみると，神経内科・老人科が主体の4認セでは平均423名/年（レンジ：126～625名/年），精神科主体の6認セでは193名/年（81～382名/年）と神経内科・老年科主体の認セが約2.2倍の数値となった。

入院者数は，県全体で当初の約430名/年から約610名/年と1.4倍に増えている．入院に関しては精神科を母体とする3病院で年間158～187名/認セの入院がある一方，精神科が母体で年間13～29名/認セの3病院がある．中核型センターを含む神経内科が中心の4病院では年間2～44名/認セと入院が少なかった．

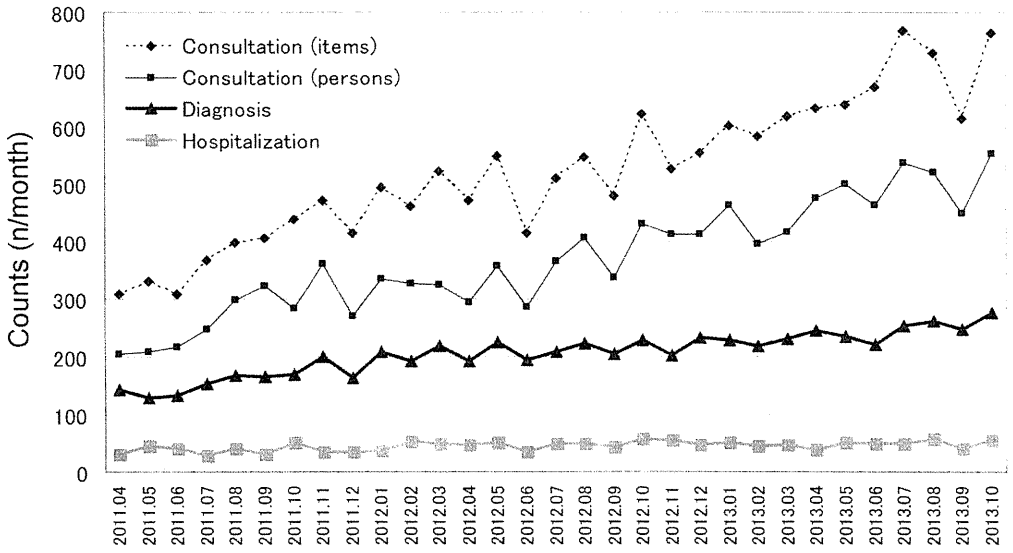

Fig. 1. Number per month of consulted items and subjects, differential diagnosis, and hospitalization in whole 10 Dementia Medical Centers in Gunma prefecture

3.2. 老年病研究所附属病院認知症疾患医療センターの実績

当認セの相談数と鑑別診断数をFig. 2 & 4に示す．対照は，当認セを除く群馬県内の地域型認セ8か所の平均とした．当認セ相談者数は，開設から伸び続け，2年半で約2倍となり，直近では月に100名（過去1年間で1,013名）からの相談を受けている．他の認セの約50名/月に比べて2倍の相談件数である．

2012年7月～2013年3月までの相談内容を分析すると（Fig. 3），電話相談は370名で，受診希望が最も多く68%を占め，病気の相談18%，病院・施設紹介9%で，介護保険などの福祉サービス相談は3%，介護相談は2%と少なかった．面接は323名で，受診希望が最も多く58%を占め，病気の相談19%，介護保険などの福祉サービス利用12%，介護相談は7%，病院・施設紹介5%であった．

当認セの鑑別診断人数は，開設から伸び続け，2年半で約3倍となり，直近では月に60名（過去1年間で625名）の診断を行っている．他の認セの20名弱と比べると3倍の診断人数である（Fig. 4）．2013年のデータから，かかりつけ医からの紹介数があるので，紹介割合を直近6か月で分析すると，当認セは40%がかかりつけ医からの紹介であった．県内の他の地域型認セでは平均51%がかかりつけ

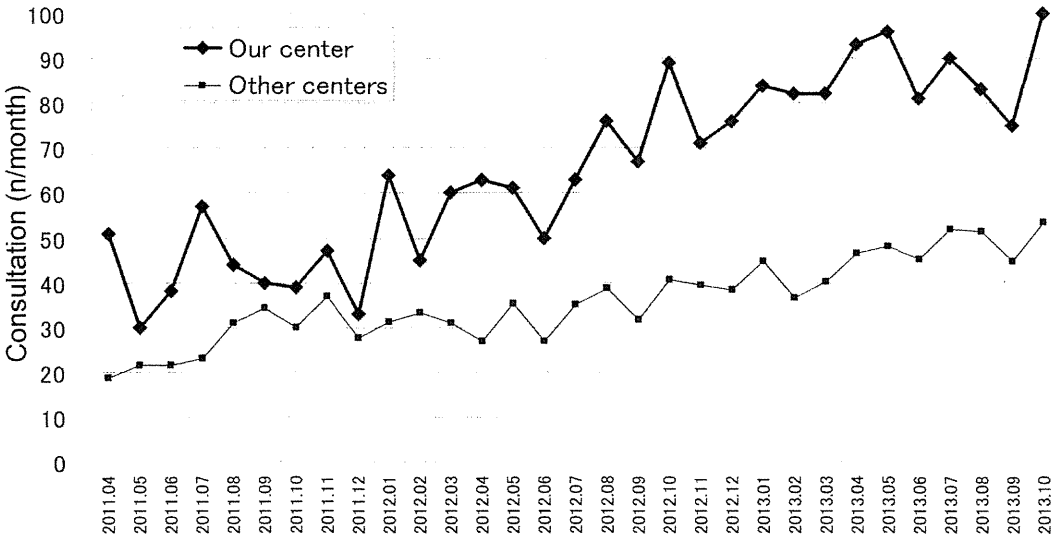

Fig. 2. Numbers of consulted subjects per month
Comparison between our center and other 8 local-type centers (mean)

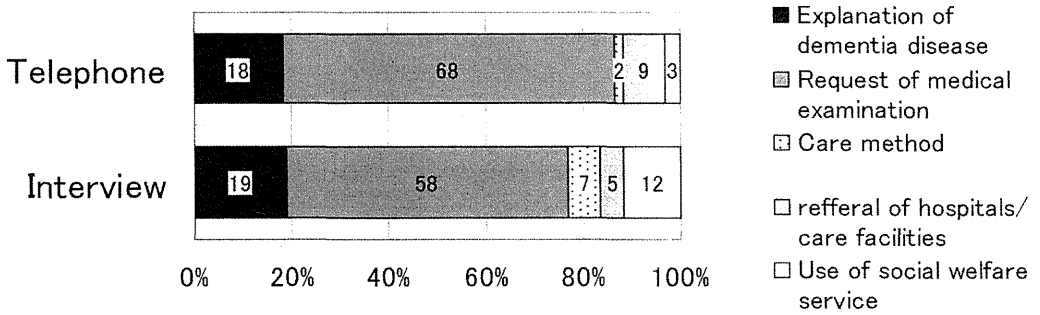

Fig. 3. Contents of consultation by phone (473 items by 370 subjects) and interview (441 items by 323 subjects)

医からの紹介であった.

また，分析期間（2012.7～2013.3）の鑑別診断は415名で，正常が23名，うつ病が3名，軽度認知障害（mild cognitive impairment；MCI）が51名，アルツハイマー型認知症（Alzheimer disease dementia；ADD）が219名，脳血管性認知症（vascular dementia；VD）が7名，レビー小体型認知症（dementia with Levy bodies；DLB）が14名，前頭側頭葉変性症（fronto-temporal lober degeneration；FTLD）が12名，他の認知症を伴わない正常圧水

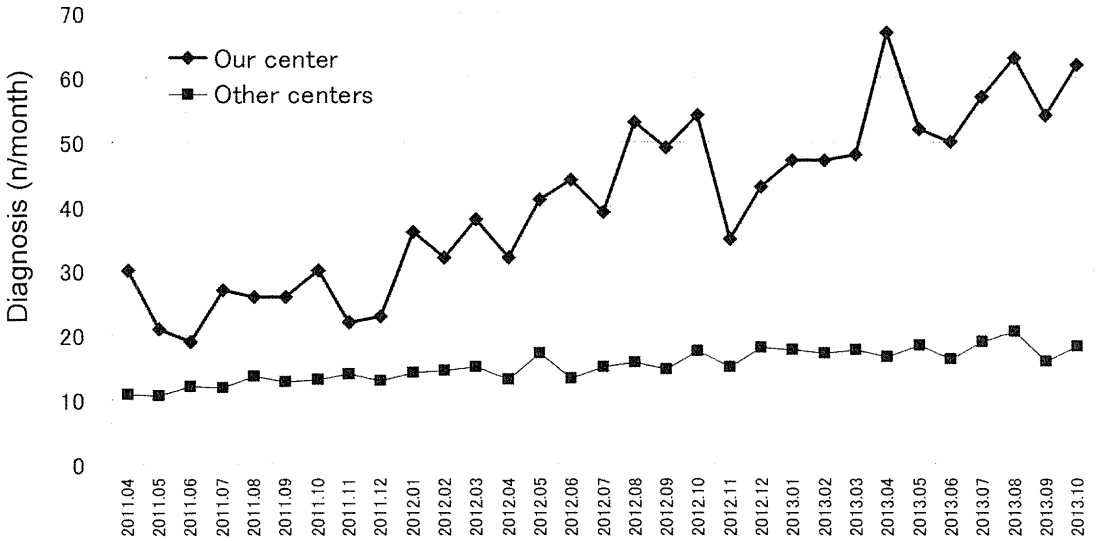

Fig. 4. Numbers of diagnosed subjects per month
Comparison between our center and other 8 local-type centers (mean)

Table 1. Result of differential diagnosis (n=415)

Diagnosis	Cases n=415	% (total)	% (dementia)
Normal	23	5.5%	
Mild cognitive impairment (MCI)	51	12.3%	
Alzheimer disease dementia (ADD)	219	52.8%	74.0%
ADD+VD	18	4.3%	6.1%
Vascular dementia (VD)	7	1.7%	2.4%
ADD+DLB	6	1.4%	2.0%
Dementia with Levy bodies (DLB/PDD)	14	3.4%	4.7%
Fronto-temporal lober degeneration	12	2.9%	4.1%
Normal pressure hydrocephalus (pure)*	12	2.9%	4.1%
Dementia, un-classified	8	1.9%	2.7%
Cerebro-vascular disease	16	3.9%	
Depression	3	0.7%	
Others	26	6.3%	
Dementia total	296	71.3%	100%

*Complication with other type of dementia was excluded